Validation of Satellite Precipitation Estimates over the Congo Basin

S. E. NICHOLSON AND D. KLOTTER

Department of Meteorology, Florida State University, Tallahassee, Florida

L. ZHOU AND W. HUA

University at Albany, State University of New York, Albany, New York

(Manuscript received 15 June 2018, in final form 17 January 2019)

ABSTRACT

This paper evaluates nine satellite rainfall products and the Global Precipitation Centre Climatology (GPCC) gauge dataset over the Congo basin. For the evaluation the reference dataset is a newly created, gridded gauge dataset based on a gauge network that is more complete than that of GPCC in recent years. It is termed NIC131-gridded. Gridding was achieved via a climatic reconstruction method based on principal components, so that reliable estimates of rainfall are available even in the data-sparse central basin. The satellite products were evaluated for two locations, the Congo basin and areas on its eastern and western periphery (termed the ''east plus west'' sector). The station density was notably higher in the latter region. Two time periods were also considered: 1983–94, when station density was relatively high, and 1998–2010, when station density was much lower than during the earlier period. Several products show excellent agreement with the NIC131-gridded reference dataset. These include CHIRPS2, PERSIANN-CDR, GPCP 2.3, TRMM 3B43, and, to a lesser extent, GPCC V7. RMSE for the period 1983–94 in the east plus west sector is on the order of 20 mm month^{-1} for GPCC V7 and 20–30 mm month^{-1} for the other products. The compares with 40–60 mm month^{-1} for the most poorly performing products, African Rainfall Climatology version 2 (ARCv2) and CMAP. Over the Congo basin, RMSE for those two products is about the same as in the east plus west sector but is on the order of 30–40 mm month^{-1} for the better-performing products. In all cases, the performance of the 10 products evaluated is notably poorer in recent years (1998–2010), when the station network is sparse, than during the period 1983–94, when the dense station network provides reliable estimates of rainfall. For the more recent period RMSE is on the order of 30–40 mm month^{-1} for the best-performing products in the east plus west sector but only slightly higher over the Congo basin. All products do reasonably well in reproducing the seasonal cycle and the latitudinal gradients of rainfall. Estimates of interannual variability show more scatter among the various products and are less reliable. Overall, the most important results of the study are to demonstrate the strong impact that actual gauge data have on the various products and the need to have access to such gauge data, in order to produce reliable rainfall estimates from satellites.

1. Introduction

The Congo basin encompasses the world's second largest area of tropical rain forest (Fig. 1). Unfortunately, the well-being of the forest is being challenged by declining rainfall, potential long-term climate change, and human activities such as deforestation. An understanding of the changes and their implications is hindered by the lack of available in situ data in recent years and the lack of in-depth understanding of meteorological processes underlying climate variability in the region.

This region captured the interest of the meteorological community when data from the Tropical Rainfall Measuring Mission (TRMM) satellite showed it to be the site of the world's most intense thunderstorms (Zipser et al. 2006). Since that time, the number of studies of the region's meteorology has continually increased. Most have centered on synoptic systems, convection, and other intraseasonal phenomena (Nguyen and Duvel 2008; Jackson et al. 2009; Gu 2009; Vondou et al. 2010a,b; Laing et al. 2011; Sandjon et al. 2012, 2014a,b; Kamsu-Tamo et al. 2014; Sinclaire et al. 2015; Berhane et al. 2015; Soula et al. 2016; Zebaze et al. 2017). Only a handful have focused on the prevailing general circulation (Nicholson and Grist 2003; Pokam et al. 2012, 2014; Dezfuli et al. 2015; Neupane 2016; Cook and Vizy 2016) and even the factors producing the seasonal cycle are poorly understood (Nicholson 2018). Recent studies have focused on

Corresponding author: S. E. Nicholson, snicholson@fsu.edu

DOI: 10.1175/JHM-D-18-0118.1

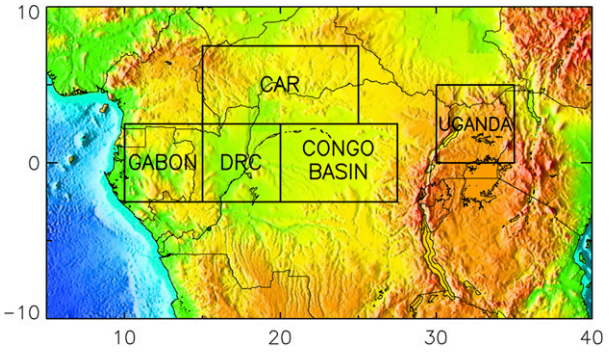

FIG. 1. Basin area and sectors used in evaluating interannual variability.

rainfall variability (Samba and Nganga 2012; Samba et al. 2008) and factors driving it (Todd and Washington 2004; Balas et al. 2007; Jackson et al. 2009; Dezfuli 2011; Dezfuli and Nicholson 2013; Nicholson and Dezfuli 2013; Diem et al. 2014; Zhou et al. 2014; Hua et al. 2016, 2018; Dyer et al. 2017).

These studies have clearly demonstrated the importance of the equatorial Walker-type circulation over the Congo basin (e.g., Neupane 2016; Cook and Vizy 2016; Dezfuli et al. 2015) in regulating the year-to-year variability of rainfall in the region (e.g., Dezfuli and Nicholson 2013; Nicholson and Dezfuli 2013; Hua et al. 2016, 2018). However, there is little consensus on the factors driving this circulation. Although tropical SSTs appear to be linked to rainfall variability, there are diverse conclusions concerning the relative importance of the Atlantic (e.g., Hirst and Hastenrath 1983; Todd and Washington 2004; Balas et al. 2007; Diem et al. 2014) versus the Indo-Pacific (e.g., Pokam et al. 2014; Hua et al. 2016, 2018; Dyer et al. 2017). Moreover, rainfall variability in many parts of the region shows little association with SSTs (Dezfuli and Nicholson 2013; Nicholson and Dezfuli 2013).

What does clearly emerge from the various studies is that factors in rainfall variability vary tremendously within equatorial Africa and that the regionalization of the factors and the factors themselves vary by season. Moreover, they may be changing in time as the tropical oceans warm (Hoell and Funk 2013). To unravel the various factors and to potentially predict future changes, a spatially detailed picture of rainfall in the region is required. This was once available, as thousands of stations were operative in equatorial Africa in the mid-twentieth century. However, in most countries of equatorial Africa, and especially in Angola and the Democratic Republic of the Congo (DRC), the networks have continually declined since the 1970s or 1980s. While, in principle, satellite data now provide the needed spatial detail, the available satellite products have generally been validated only over eastern equatorial Africa, a region very different climatically from the Congo basin. Two validations that did emphasize the Congo basin found large discrepancies between gauge and satellite data (McCollum et al. 2000; Yin et al. 2004). Negron Juarez et al. (2009) and Sun et al. (2018) similarly found satellite estimates of rainfall to be poor over equatorial Africa, with wide discrepancies among the various satellite products. This was particularly the case for the Congo basin.

The purpose of this article is to use a dense gauge dataset to validate satellite rainfall estimates over central and western equatorial Africa. The article commences with a description of satellite products to be evaluated (section 2) and continues with a review of past validation efforts that focused on East Africa or included parts of the Congo basin (section 3). A description of the gauge dataset used here and the methodology of the validation are described in section 4. Results are presented for seasonal and monthly rainfall estimates (section 5). An important aspect of the work is comparing the satellite performance during a period with relatively high gauge station density (1983–94) with the performance during a more recent period (1998–2010) when gauge density over the basin itself is extremely low. Conclusions on the importance of the gauge data and guidance for use of the various products are presented in section 6.

2. Precipitation products evaluated

In this study, nine satellite precipitation products and the Global Precipitation Climatology Centre (GPCC) V7 gauge dataset, produced by the German Weather Service (DWD) under the auspices of the WMO, are evaluated. Table 1 summarizes characteristics of these products, including the extent to which gauge data, such as that from the Global Telecommunications System (GTS) or GPCC, have been incorporated into each product or used to adjust it. The satellite products considered are those that have been used extensively to study rainfall over Africa. Several are based only on thermal infrared (IR) retrievals. These include Climate Hazards Group Infrared Precipitation with Station Data (CHIRPS2); Tropical Applications of Meteorology Using Satellite Data and Ground-Based Observations (TAMSAT3), African Rainfall Climatology version 2 (ARCv2), and Precipitation Estimation from Remotely Sensed Information Using Artificial Neural Networks (PERSIANN-CDR). Other products merge thermal IR and microwave data: Tropical Rainfall Measuring Mission (TRMM) 3B43; Climate Prediction Center (CPC) morphing technique (CMORPH CRT); CPC Merged

TABLE 1. The 10 rainfall products evaluated in this study.

Product	Start	End	Resolution		Gauge use
			Spatial	Temporal	
ARCv2	January 1983	Present	0.1°	Daily	Merge–GTS
CHIRPS2	1981	2015	0.05°	Daily	Merge
CMAP	January 1979	Present	2.5°	Pentad	Merge
CMORPH CRT	December 2002	Present	8 km	Subdaily	Adjusted
GPCC V7	1901	2013	0.5°	Monthly	Gauge only
GPCP 2.3	January 1979	Present	2.5°	Monthly	Merge
PERSIANN-CDR	January 1983	Present	0.25°	Subdaily	Adjustment
RFE 2.0	January 1983	Present	0.1°	Daily	Merge–GTS
TAMSAT V3	January 1983	Present	4 km	Daily	Adjustment
TRMM 3B43 V7	January 1998	Present	0.25°	Monthly	Merge

Analysis of Precipitation (CMAP); and CPC Rainfall Estimation (RFE) 2.0; and the Global Precipitation Climatology Project (GPCP 2.3). Three of the products (ARCv2, RFE 2.0, TAMSAT3) cover solely the African continent and were produced primarily for drought monitoring. All are merged with gauge data or utilize gauge data for bias adjustment. Although the products vary considerably in spatial and temporal resolution, all have been aggregated to the same temporal and spatial scales of this study, monthly at 2.5° and 5.0°. Most of the products are available since 1979 or 1983. However, TRMM 3B43, RFE 2.0, and CMORPH CRT are available only since 1998.

The GPCC version 7 used here is monthly and has a spatial resolution of 2.5° (Schneider et al. 2015). It should be noted that GPCC and the reference dataset used for validation, termed NIC131, are not completely independent products. Most of the NIC131 data up through 1998 were incorporated into GPCC. As a result, the correlation of the two sets during the 1983–94 period is almost perfect. Differences arise from the method of gridding, as opposed to differences in the raw station values. After 1998, GPCC relies mostly on data transmitted through the GTS, while NIC131 includes numerous updates obtained directly from the African meteorological services. Although the gauge network for both products is extremely sparse over the Congo basin during the 1998–2010 validation period (Fig. 2), the contrast in the available data during that period adds some degree of independence. Moreover, a spatial reconstruction method based on principal components (see section 4) has been used to fill in gaps in NIC131 in recent years. That dataset, termed NIC131-gridded, provides a dataset over the Congo basin that is largely independent of the GPCC V7 product. This is important because many of the satellite rainfall products incorporate GPCC data to some degree, yet many validation studies use GPCC as the reference data. Thus, the NIC131-gridded dataset allows for a more independent and adequate validation of the various satellite products.

The TRMM satellite was a joint mission between NASA and the Japanese Aerospace Exploration Agency. It was specifically designed to measure tropical rainfall globally. The product used here, 3B43 V7, is a monthly accumulation of 3B42 V7 product that merges precipitation estimates from several passive microwave products with microwave-calibrated infrared-based precipitation estimates and then performs bias adjustment using monthly accumulated rain gauge analysis from GPCC (Huffman et al. 2007, 2010; Huffman and Bolvin 2014). TRMM 3B43 is a monthly product with a spatial resolution of 0.25°.

GPCP was originally produced by NASA's Goddard Space Center (Adler et al. 2003) but is now being produced by NOAA–University of Maryland. Like TRMM 3B43, it merges microwave and infrared estimates from polar orbiting and geostationary satellites but from a different constellation of sensors. It is also a monthly product but has a spatial resolution of 2.5°. GPCP 2.3 is available since 1979, and it does not utilize data from TRMM instruments, which do not commence until 1998. It is adjusted with gauge data from GPCC.

NOAA's CPC provides two rainfall products for Africa only, RFE and ARC. RFE 2.0 is based on three satellite products (Xie and Arkin 1996, 1997; Love et al. 2004); daily gauge data from the GTS are used to correct the bias. The satellite products include 1) IR data from the Geosynchronous Operational Environmental Satellite (GOES) precipitation index (GPI), 2) passive microwave estimates from the Special Sensor Microwave Imager (SSM/I) and 3) Advanced Microwave Sounding Unit (AMSU) microwave estimates of rainfall. The GPI is based on IR cloud-top temperature from Meteosat, which is centered over Africa. A daily product is produced with a spatial resolution is 0.1°. The ARCv2 (version 2) product has the same spatial and temporal resolution. The main difference between REF

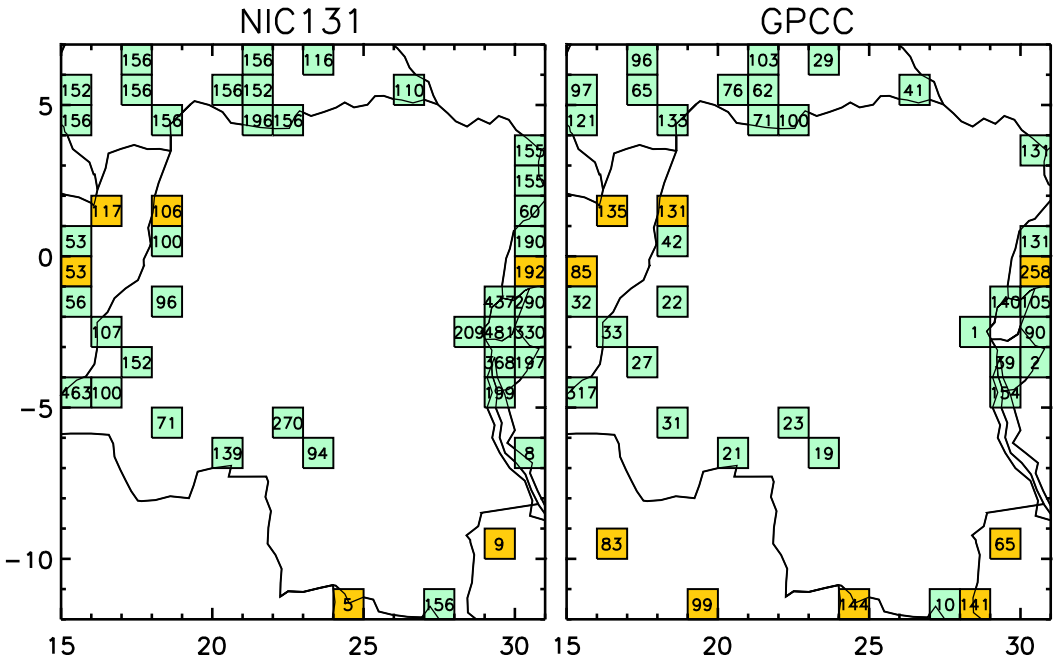

FIG. 2. Total number of months with available rainfall records during the period 1995–2012 for any grid box with data in (left) NIC131 or (right) GPCC. Grid boxes in orange are those with a greater number of records in GPCC than in NIC131.

2.0 and ARCv2 data is that the algorithm used to produce the latter does not contain microwave data (Novella and Thiaw 2013).

CPC also provides two global products, CMORPH and CMAP. The former ''morphs'' high-quality passive microwave estimates from several low-orbiting satellites with high spatial and temporal resolution IR data to yield information for the time period between microwave sensor scans (Joyce et al. 2004). The final product is half-hourly precipitation estimates. The current study uses the CMORPH CRT product, with bias removed via comparison with gauge data (Xie et al. 2017). It is available since 1998. The raw CMORPH CRT product has been shown to have a positive bias over tropical land areas. CMAP (Xie and Arkin 1997) provides pentad and monthly analyses at a spatial resolution of 2.5°. It is based on a merger of gauge data plus five infrared and microwave satellite estimates (Xie and Arkin 1997). Satellite estimates provide the spatial pattern of rainfall and gauge data are used to calibrate the magnitude. IR data is from geostationary satellites as of 1986; previously only outgoing longwave radiation (OLR) from polar orbiting satellites was used.

CHIRPS2 (Funk et al. 2015), TAMSAT V3 (Tarnavsky et al. 2014; Maidment et al. 2013, 2017), and PERSIANN-CDR (Ashouri et al. 2015) are all based on thermal IR brightness temperature from geostationary satellites. CHIRPS2 is a result of a collaboration between the University of California at Santa Barbara and USGS. It is based on cold-cloud duration from two geosynchronous thermal IR archives produced by NOAA. One is the 1981–2008 Globally Gridded Satellite (GridSat) produced by the National Climate Data Center. The second is the 2000 to present NOAA Climate Prediction Center dataset (CPC TIR). The thermal IR data are merged with African gauge data, using ''smart'' interpolation techniques that taken the spatial correlation structure into account.

TAMSAT, produced at the University of Reading, utilizes Meteosat thermal IR data. It is based on two assumptions: that most rainfall over Africa results from convective clouds and that there is a linear relationship between cold-cloud duration and precipitation amount. The IR estimates are not merged with contemporaneous gauge data, but the product is calibrated with historical rain gauge data (Maidment et al. 2013). There are two versions of TAMSAT, with the second (TAMSAT3) designed to correct a dry-bias evident in the earlier version (Maidment et al. 2017). TAMSAT3 is used here.

PERSIANN-CDR (Ashouri et al. 2015) is also based on geostationary thermal IR brightness temperature, with a neural network approach applied to produce the precipitation estimates. The product is calibrated using NCEP–NCAR precipitation forecasts. It is bias-corrected with the GPCP precipitation product on a monthly basis, such

that PERSIANN-CDR and GPCP monthly totals are consistent. Its spatial resolution is 0.25°.

3. Prior validation of satellite rainfall products over equatorial Africa

Most of the satellite validation that has been carried out for equatorial regions of Africa is confined to East Africa, the westernmost regions considered being parts of the Rift Valley Highlands. Most validation efforts were limited to relatively small geographical areas of East Africa, such as Uganda (Diem et al. 2014; Asadullah et al. 2008; Maidment et al. 2017), northeast Tanzania (Mashingia et al. 2014), a valley in central Tanzania (Koutsouris et al. 2016), or the Lake Victoria catchment (Kizza et al. 2012). Cattani et al. (2016) examined a much broader area of East Africa, but validation was limited to a comparison with the seasonal cycle and with the relationship between rainfall and terrain. Of six products evaluated, TRMM 3B42 performed best. Numerous studies have validated satellite precipitation estimates over Ethiopia, especially in the Nile basin (e.g., Haile et al. 2013; Jacob et al. 2013; Gebremichael et al. 2014; Dinku et al. 2007, 2011a,b, 2014). However, a summer rainfall regime prevailed in regions of analysis, hence the results are not particularly relevant to the Congo basin.

For the Congo basin, two early validations (McCollum et al. 2000; Yin and Gruber 2010) raised questions about satellite precipitation estimates in the region. The latter paper noted an abrupt change around 1992 in estimates from GPCP and concluded that a change in station network caused GPCP to underestimate rainfall post-1992. In contrast, McCollum et al. (2000) concluded that GPCP overestimates rainfall over the Congo, by a factor of two. Munzimi et al. (2015) is the only recent validation of satellite precipitation estimates in the Congo basin. They solely considered TRMM and focused on improving estimates by using 12 gauges in the DRC to recalibrate the TRMM 3B42 product in this region. They also concluded that TRMM 3B43 accurately depicts Congo basin precipitation without biases.

A novel feature of that work was evaluating the satellite estimates by comparing spatial patterns of precipitation, based on a dense historical network of stations. Pombo et al. (2015) likewise used historical data (pre-1974) to validate TRMM 3B42 estimates of precipitation extremes over Angola, also a country with a vast number of historical stations but few in recent decades. Pombo and Proença de Oliveira (2015) used 18 recent Angolan stations to evaluate satellite estimates of rainfall. TRMM 3B43 was found to perform better than GPCP 2.3, PERSIANN-CDR, or CMORPH CRT. Beighley et al. (2011) noted that estimates of Congo basin rainfall from TRMM 3B42, PERSIANN-CDR and CMORPH CRT differed by a factor of two in nearly all months and in each of six subbasins of the Congo River. A comparison with model-predicted streamflow suggested that TRMM 3B42 provided the best spatial and temporal distributions and magnitudes of rainfall over the basin.

Satellite precipitation estimates over equatorial Africa have also been examined in the context of Africa-wide studies. The most extensive validation is that of Awange et al. (2016). When compared against GPCC rainfall data, TRMM 3B43 performed best among six satellite products with respect to standard error statistics [bias, root-mean-square error (RMSE), and correlation coefficients] throughout the continent. However, TRMM 3B43 is not independent of GPCC. When an alternative approach to qualifying noise and signal-to-noise ratios was applied, PERSIANN-CDR was found to perform best throughout the continent. Notably, in three products (PERSIANN-CDR, TAMSAT V3, TRMM 3B43) the signal-to-noise ratio was considerably lower over the Congo basin than elsewhere. In contrast, Serrat-Capdevila et al. (2016), examining daily rainfall statistics, found that satellite estimates of rainfall were best in the equatorial region (5°N–5°S), presumably because of the predominance of convective cloud there. Again, TRMM (TMPA) tended to perform better than either PERSIANN-CDR or CMORPH CRT, but the results varied with the rainfall parameter considered. Dezfuli et al. (2017) compared the new IMERG product, available since 2014, with TRMM throughout Africa. They noted that, despite good agreement in equatorial regions, the performance there is uncertain because of the lack of gauge data during the period in question.

4. Overview of methodology

In this study, nine satellite precipitation products and the GPCC V7 gauge-dataset are compared with rainfall estimates from a dense gauge dataset over equatorial Africa (i.e., NIC131-gridded). Validation is carried out at 2.5° and on monthly and seasonal time scales. The error statistics calculated include the random or RMSE, the systematic error or bias, and the correlation between the product and the reference gauge dataset. Taylor diagrams are used to depict the correlation, RMSE, and the standard deviation of the estimates. Evaluation of the 10 products is also made by examining the ability to reproduce mean meridional transects, the seasonal cycle, and interannual variability. Sample maps for two

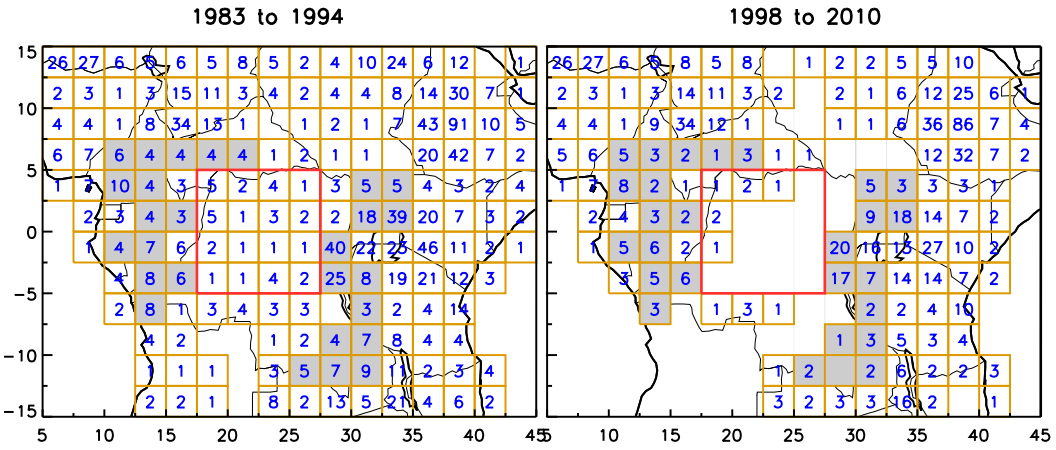

FIG. 3. Stations available in NIC131 in any year during 1983–94 and 1998–2010. Numbers indicate stations per grid box. Gray shading indicates the east plus west analysis sector; the red box indicates the central basin analysis sector.

individual months are presented to provide an overview and direct comparison of the products.

The reference gauge dataset (i.e., NIC131) is from an Africa-wide archive compiled by the first author (e.g., Nicholson et al. 2018a). This 2.5° gridded dataset (i.e., NIC131-gridded) was created by applying a spatial reconstruction technique based on principal component analysis (Nicholson et al. 2018b). This approach has the advantage that, in contrast to most approaches such as kriging, it does not assume a linear relationship between missing stations/grid points and the nearest available value or values. When gaps are as large as in the Congo basin, the linear relationship is very unlikely to hold. The principal components recognize the complexity of the spatial relationships, taking the spatial correlation structure into account. Also, it was determined that if three or more gauges were available, a simple station average would adequately represent rainfall within the grid box. For that reason, spatial reconstruction was applied only to grid boxes that included fewer stations. For those with three or more stations, the value for the grid box is the simple average of gauge data. That dataset extends from 1921 to 2014 and covers most of the area between 12.5°N and 15°S.

In terms of a reference dataset, GPCC is used in many validation studies. We argue that NIC131-gridded is a more appropriate reference dataset. For one, since most of the satellite products evaluated here incorporate GPCC to some extent, they are not really independent of it. As indicated, prior to the 1990s GPCC and NIC131 relied upon the same gauge dataset, but in recent years there is a much greater degree of independence. Also, in recent years NIC131-gridded has more gauge data than does GPCC over and around the Congo basin. Further, NIC131-gridded was validated with raw station data over the period 1973–2010, using a cross-validation technique, and its performance was shown to be excellent. The spatial reconstruction approach was tested against the more commonly used kriging and was found to give far superior results in this region, with the RMSE for kriging being roughly twice that for the spatial reconstruction technique.

The validation of the satellite products is complicated by the decline in the station network in the late 1980s, combined with the fact that three of the satellite products are first available in 1998 or later. For this reason, validation is carried out over two separate periods, 1983–94 and 1998–2010, with somewhat different approaches. The decision to end the first validation period at 1994 is based on the fact that the number of stations in the Democratic Republic of the Congo, the heart of the Congo basin, diminishes rapidly after that time. Figure 3 shows the available stations during these two periods. During the period 1983–94 the station network is dense and it changes relatively little from year to year.

Two separate sectors are also considered in the validation, one with a relatively dense gauge network and one in which most data are a result of spatial reconstruction. An examination of the station network year by year suggested that the grid boxes shaded in gray in Fig. 3 would generally meet the three-station criterion during the 1983–94 period. These are concentrated on the eastern and western periphery of the Congo basin and are analyzed collectively and the sector termed ‘‘east plus west.’’ Note that grid boxes which include large portions of the Atlantic or a lake are excluded, even if adequate gauge stations are available. The region outlined in red in Fig. 3, henceforth termed the ‘‘central basin,’’ has few stations in any time period and is considered separately in the various analyses.

For the east plus west sector, the error analyses for 1983–94 are based only on the subset of NIC131 grid boxes with three or more stations. That is, the reference dataset for the error analyses excludes any spatially reconstructed values. To enhance the number of stations going into the spatial average, those within 0.1° of the boundaries of a 2.5° grid box were incorporated into the station average for the grid box. The number of adequate grid boxes varies from month to month and from year to year. Note that most grid boxes contained at least four stations, so that a comparison of results based on three versus four stations in defining ''adequate'' shows little difference. The three-station criterion allows for the inclusion of a greater number of grid boxes.

As noted, within the Congo central basin, few station records are available even in the period 1983–94. To examine the performance of satellite products within the basin itself, it was necessary to utilize the full, reconstructed NIC131-gridded dataset.

The second validation period is 1998–2010. The decision to commence the validation in 1998 was based on the fact that some products, such as TRMM, become available only in 1998. During this period only the "reconstructed" NIC131-gridded dataset is utilized. It provides spatially and temporally continuous coverage. In its creation, statistical reconstruction was applied only to grid boxes with fewer than three gauge stations. Hence, for the study area that includes the eastern plus western grid boxes in Fig. 3, the grid boxes have undergone little statistical manipulation, so that results are directly compared to those obtained for 1983–94. For the 1998–2010 period, all nine satellite products plus GPCC V7 are evaluated, using NIC131-gridded as the reference dataset.

As indicated above, the error statistics include RMSE, bias, and linear correlation r. These are computed as

$$\text{bias} = \sum_{i=1}^{N} S_i - \sum_{i=1}^{N} G_i,$$

$$\text{RMSE} = \sqrt{\frac{1}{N}\sum_{i=1}^{N}(S_i - G_i)^2}, \qquad \text{and}$$

$$r = \frac{N\left(\sum_{i=1}^{N} S_i G_i\right) - \left(\sum_{i=1}^{N} S_i\right)\left(\sum_{i=1}^{N} G_i\right)}{\sqrt{\left[N\sum_{i=1}^{N} S_i^2 - \left(\sum_{i=1}^{N} S_i\right)^2\right]\left[N\sum_{i=1}^{N} G_i^2 - \left(\sum_{i=1}^{N} G_i\right)^2\right]}},$$

where G_i is the value of rainfall in NIC131-gridded, S_i is the value of rainfall in the satellite product or GPCC V7, and N is the total sample size. The calculations are made over an array that includes each adequate grid box within the indicated sector and each of the years considered. These statistics are calculated for each month and for four multimonth seasons: January–March (JFM), April–June (AMJ), July–September (JAS), and October–December (OND).

5. Results

This study commences with a cursory look at spatial patterns of rainfall in two individual months of the year 2001, based on each of the nine satellite products and three gauge products (Fig. 4). Examples are shown for March and November of the year 2001. Those months are shown because they are the months of maximum Congo basin rainfall during the boreal spring and boreal fall rainy seasons. The figure also includes the patterns based on GPCC V7 and NIC131-gridded, as well as the rainfall at the individual stations available in these months. These clearly illustrate the large disparity in satellite estimates of rainfall over equatorial Africa.

In March (Fig. 4a), the NIC131-gridded estimates show four notable features. The first is a strong north–south gradient, with rainfall on the order of 200–300 mm in the south and generally 10–100 mm in the north around 5°–8°N. The other features are a local minimum around 20°–30°E far to the south, a strong maximum in the far western equatorial region, and a second equatorial maximum around 30°E. Each of these features are evident to some degree in CHIRPS2, GPCC V7, GPCP 2.3, PERSIANN-CDR, TRMM 3B43, and TAMSAT V3. CHIRPS2, however, shows a comparatively weak western equatorial maximum and a very strong maximum in the southern latitudes. That pattern is the one most similar to that of NIC131-gridded. In contrast, CMAP lacks the north–south gradient and shows a strong east–west gradient in the equatorial latitudes; ARCv2 misses most of the southern maximum, as does RFE 2.0.

In November (Fig. 4b) the maximum is not in the southern latitudes but in the equatorial region. A separate maximum is evident far to the west in the equatorial latitudes; a third is apparent far to the east over central Kenya. A nearly rainless region is evident in central Tanzania. These same features are seen in TRMM 3B43, PERSIANN-CDR, GPCC V7, GPCP, TAMSAT V3, and to a lesser extent in CHIRPS2. ARCv2, RFE 2.0, and CMORPH CRT all show a much larger rainless area covering most of Tanzania and northern Mozambique. CMAP lacks the western equatorial maximum. Overall, the equatorial maximum is relatively weak in CHIRPS2, RFE 2.0, and CMORPH CRT, but perhaps anomalously strong in PERSIANN-CDR and TRMM 3B43.

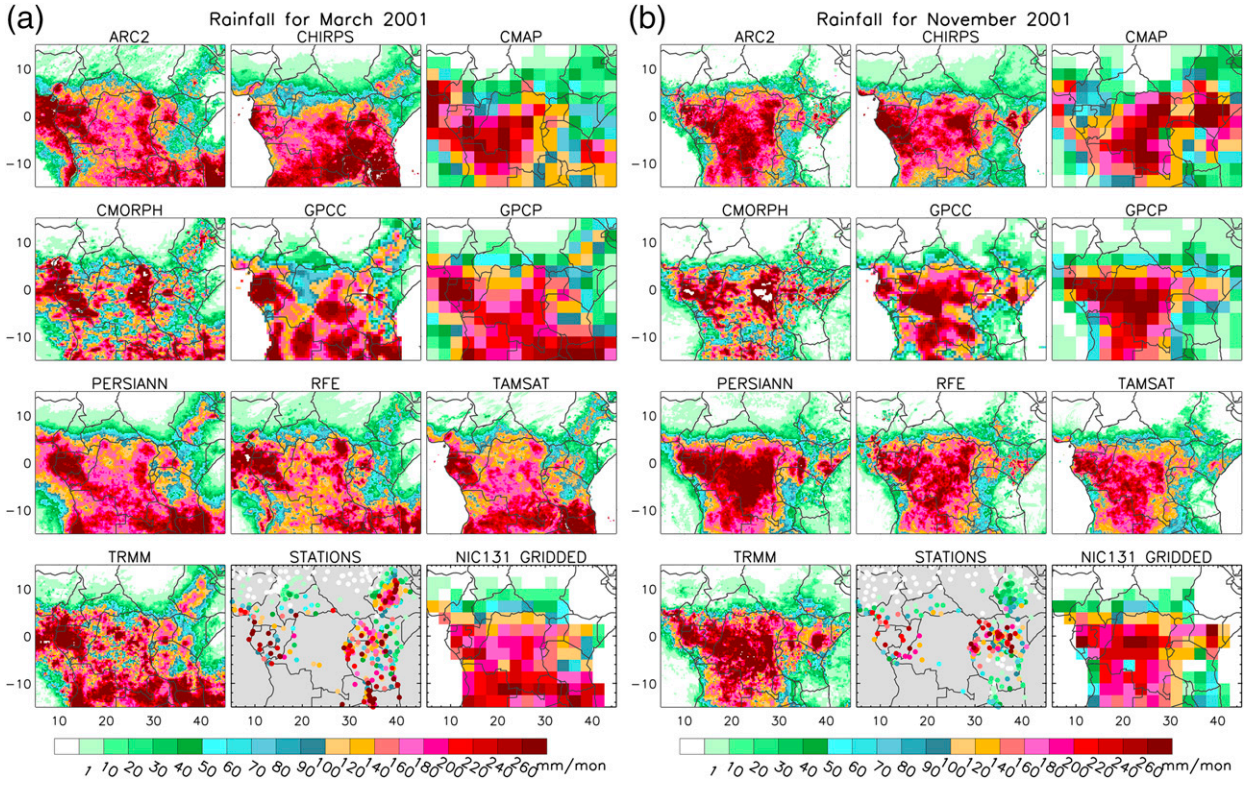

FIG. 4. Maps of rainfall (mm month^{-1}) for (a) March and (b) November 2001.

a. Error statistics

1) TAYLOR DIAGRAMS

The 10 products are compared for each month and four seasons using Taylor diagrams (Taylor 2001). The Taylor diagrams illustrate the correlation of each product with the NIC131-gridded reference dataset (i.e., the ''observed'' in the diagram), the variance of the 10 products and the observed, and the RMSE compared with the observed. It should be emphasized that these estimates are relative to NIC131-gridded and not absolute. The error in the NIC131-gridded reconstructions is on the order of 10% (Nicholson et al. 2018b).

In the diagrams for the east plus west sector for the 1983–94 period (Fig. 5) three tendencies are evident. 1) The variance of the estimates shows little variation among the 10 products and tends to be similar to that of the reference dataset. 2) The performance of most of the products does not vary greatly from month to month. 3) Certain products tend to be outliers, especially during the rainy season months of March, April, May, October, and November. A visual scan of the diagrams suggests that ARCv2 is an outlier in nearly all cases, CMAP is an outlier in most cases, and TAMSAT V3 is an occasional outlier. This is evident both in terms of correlation with the reference data and in terms of standard deviation. Even in those cases, however, the correlation with observed is never less than 0.7 and is generally greater than 0.9. For the other products, the correlation with the observed is on the order of 0.9–0.95 in nearly all cases. The highest correlations tend to be with GPCC V7 and GPCP 2.3. As mentioned, this is not surprising since GPCC incorporates NIC131 data during this time period and GPCP is strongly dependent on GPCC.

The results are different for the central basin during the 1983–94 period (Fig. 6). The spread of the satellite products is much greater and the correlation with NIC131-gridded is much weaker, especially in the wettest months. Typical correlations are as low as 0.3–0.4 in April and October and 0.5–0.6 in May. As for the east plus west sector, there are clusters of similarly performing products, including CHIRPS2, GPCC V7, PERSIANN-CDR, and occasionally TAMSAT V3. ARCv2, CMORPH CRT, CMAP and often TAMSAT V3 tend to be outliers, compared to those clusters. Notably, correlation between GPCC V7 and NIC131-gridded is low in some months, on the order of 0.4–0.5 in April, May, and October. Unfortunately, it is impossible to ascertain whether GPCC V7 or NIC131-gridded performs better in this region. This question will be considered later.

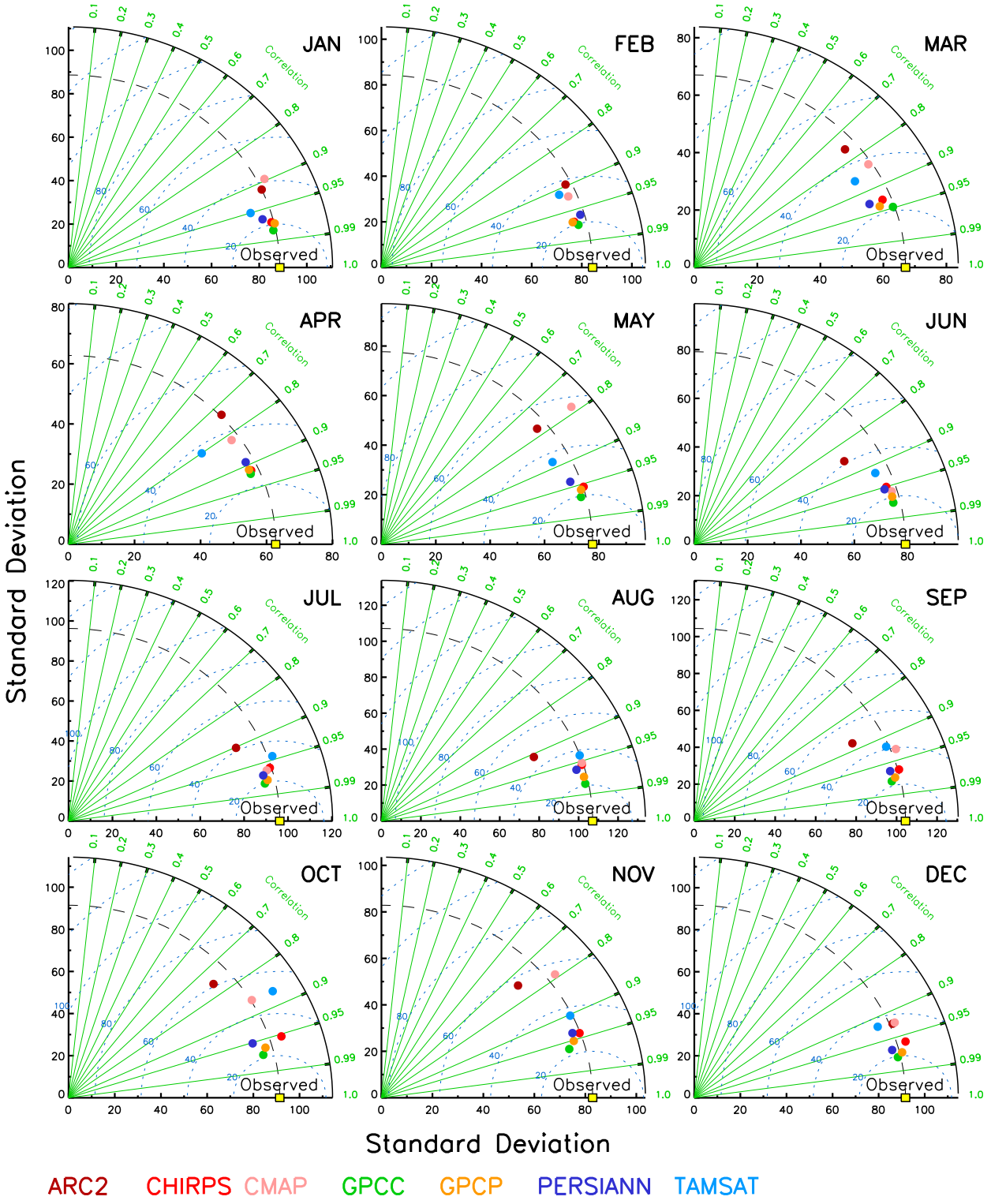

FIG. 5. Taylor diagrams for 1983–94 for the east plus west sector. "Observed" refers to the NIC131 dataset. In this case, only grid boxes with 3 or more stations are considered. The correlations are based on roughly 206 points. The *x* and *y* axes are standard deviation; the thin green dashed lines are the RMSE.

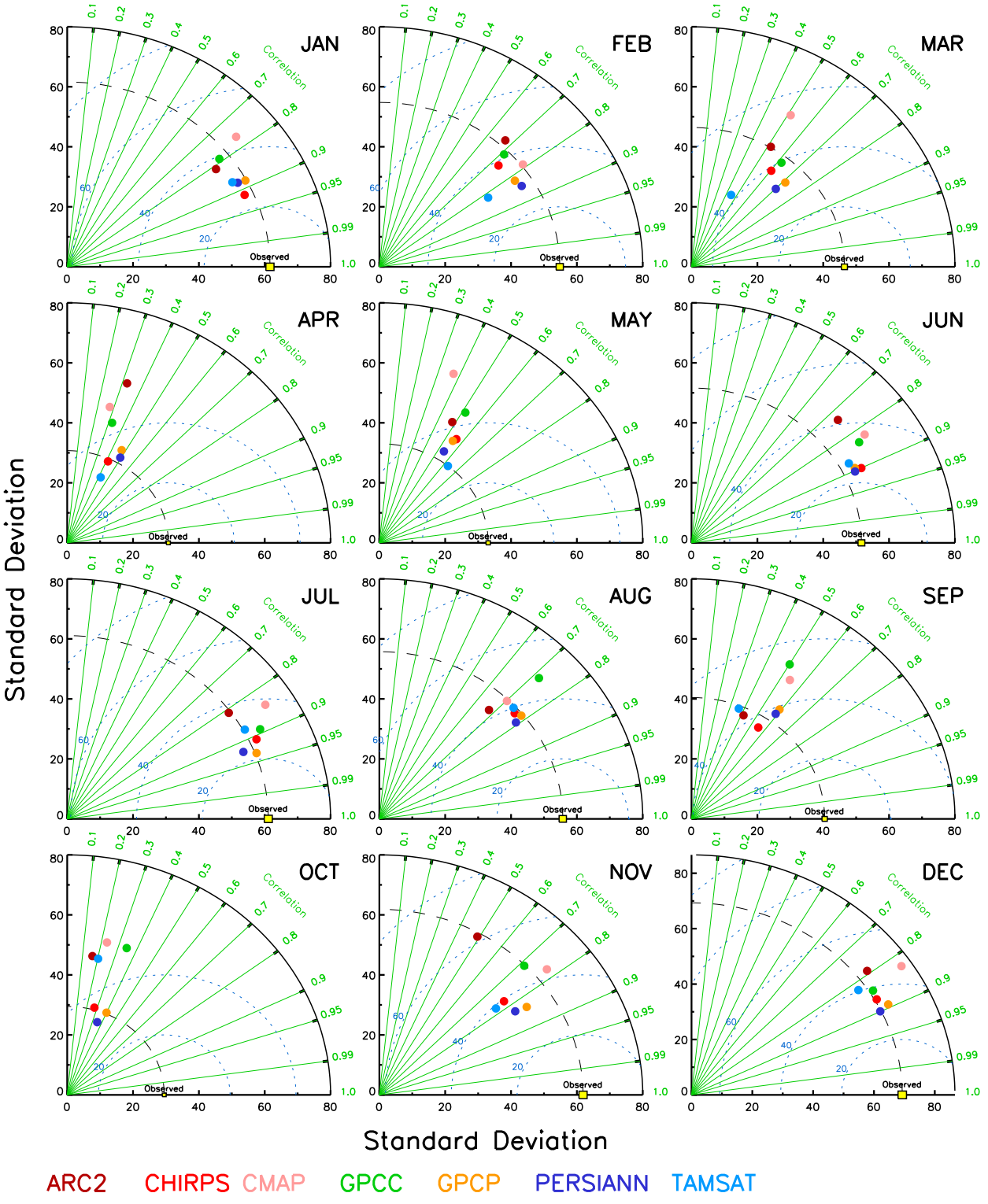

FIG. 6. Taylor diagrams for 1983–94 for the central basin. Analysis uses the "reconstructed" version of NIC131, so that all grid boxes in this sector are included in each month and year. The correlations are based on roughly 350 points. The *x* and *y* axes are standard deviation; the thin green dashed lines are the RMSE.

The diagrams for the period 1998–2010 (Figs. 7, 8) show greater disparity among the 10 products in terms of both the correlation with the observed and the variance of the estimates. For the east plus west region the correlation of most products with the reference dataset is still strong, but on the order of 0.7–0.9 (higher in the dry months). However, in April correlations are universally lower, on the order of 0.6–0.8. The standard deviation of each of the products is also much lower in April than in the other months. ARCv2, RFE 2.0, CMAP, and CMORPH CRT are frequent outliers. During this period, CHIRPS2 is clearly closest to the observed in nearly all cases and GPCC is an occasional outlier. The correlation between CHIRPS2 and the reference dataset is generally between 0.8 and 0.9, and the standard deviation of CHIRPS2 is very close to that of the reference dataset in all months. Note that the station network in the NIC131 reference dataset is not substantially different from that of the 1983–94 period (Fig. 3) and spatial reconstruction was applied to few grid boxes. Hence, the reference dataset is reliable.

The results for the central basin during 1998–2010 show much weaker correspondence with NIC131-gridded and much greater spread among the 10 products, particularly with respect to the standard deviation of the estimates. As with the east plus west sector, CHIRPS2 shows the best correlation with NIC131-gridded and the correlation is on the order of 0.7–0.9 in most months. However, it is as low as 0.3 in April and 0.4 in October. The correlation with most other products in those months is even weaker.

The greater disparity of the estimates in the central basin and during the period 1998–2010 compared to 1983–94 is not surprising. Each of the products is dependent on gauge data to some extent, but the anchoring by gauge stations is generally weak in the central basin and weaker during the later period, a consequence of the paucity of observations. This means that differences in the input satellite datasets and the algorithms utilized play a greater role during 1998–2010 than during 1983–94. Further influencing the correlations is the greater error in the NIC131-gridded dataset over the central basin during the 1998–2010 period, a result of spatial reconstruction being used to fill in gaps. Overall, the very diverse results for the various satellite products and GPCC V7 show the importance of having a dense gauge data network as an input to the product. The question still remains whether NIC131-gridded or GPCC is the more reliable gauge dataset for this region.

Figure 9 compares the results for both sectors and time periods at the seasonal level. The seasonal aggregation serves to reduce via the averaging process much of the random error in estimates. As seen with monthly data, ARCv2, CMAP, and CMORPH CRT are frequently outliers. The remaining discussion will focus on the other products. For the east plus west sector the results are generally excellent for the 1983–94 period. With the exception of the outliers, the correlation with the reference rainfall dataset is generally 0.9–0.98 and there is little scatter among the results for the various products and there is little difference in the results among the four seasons. For the 1998–2010 period the performance of the products in the east plus west sector is weaker but still good. There is more scatter among the 10 products and the correlations vary considerably for the different seasons. For most products they are on the order of 0.9–0.95 or higher for JFM and JAS, the driest seasons, and on the order of 0.8–0.8 for AMJ and OND.

As to be expected, there is greater scatter among the 10 products for the central basin and correlations with the reference dataset are lower. This is true for both time periods. Again, CMORPH CRT is consistently an outlier and ARCv2, CMAP, and RFE 2.0 are frequent outliers. For the other products, there is generally little scatter for the standard deviations and the correlations tend to be on the order of 0.7–0.9. Results for 1983–94 and 1998–2010 are fairly similar. The exception is AMJ of the later period, when correlations are on the order of 0.65 for one cluster of products (TRMM 3B43, PERSIANN-CDR, CMAP, GPCP 2.3, and GPCC V7) and on the order of 0.7–0.8 for a second cluster (ARCv2, TAMSAT V3, CHIRPS2, and RFE 2.0).

2) RMSE OF MONTHLY ESTIMATES

The RMSE is summarized in Fig. 10 for monthly estimates. It is shown for both sectors and time periods. There are consistent differences among the products for the east plus west sector during the 1983–94 period. RMSE is lowest for GPCC V7 in each month and season, generally being on the order of 20 mm month^{-1}. This is not surprising since the reference gauge set and GPCC V7 include mainly the same station records during this period. The RMSE is only marginally higher for GPCP 2.3, PERSIANN-CDR, and CHIRPS2, generally on the order of 20–30 mm month^{-1}. In contrast, RMSE is consistently (10 of 12 cases) highest for ARCv2 and is on the order of 40–50 mm month^{-1}. It also tends to be high for CMAP and TAMSAT V3.

For RMSE over the central basin during 1983–94 there is less spread among the 10 products, which is surprising in view of the lower gauge station density in this region. In most months RMSE is on the order of 30–40 mm. It tends to be lowest for CHIRPS2, PERSIANN-CDR, and TAMSAT V3 and highest for ARCv2 and CMAP. GPCC V7 RMSE is also relatively low but nearly twice as great as in the other sector.

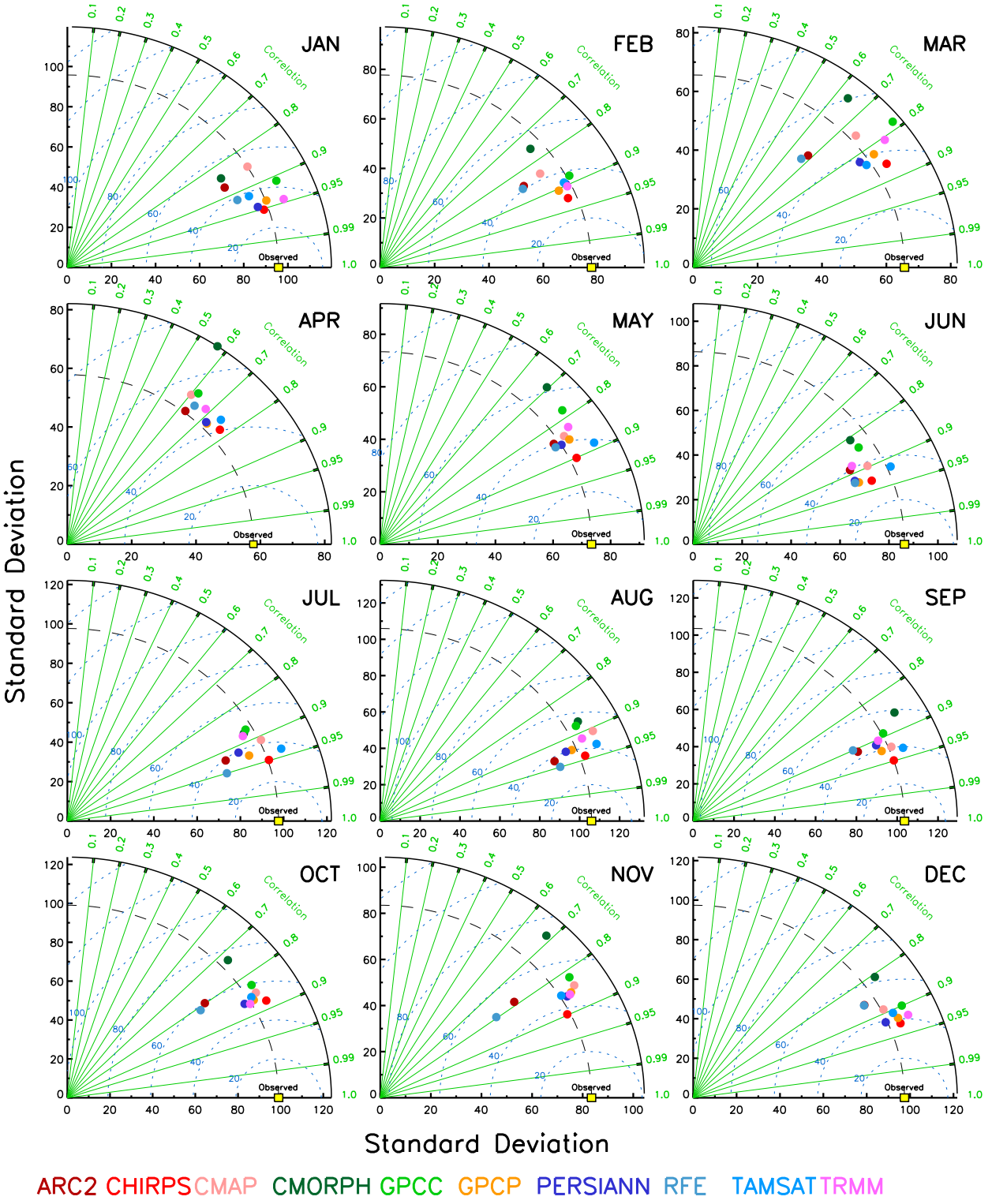

FIG. 7. Taylor diagrams for 1998–2010 for the east plus west sector. "Observed" refers to the NIC131 dataset. Analysis uses the "reconstructed" version of NIC131, so that all grid boxes in this sector are included in each month and year. The correlations are based on roughly 200 points. The *x* and *y* axes are standard deviation; the thin green dashed lines are the RMSE.

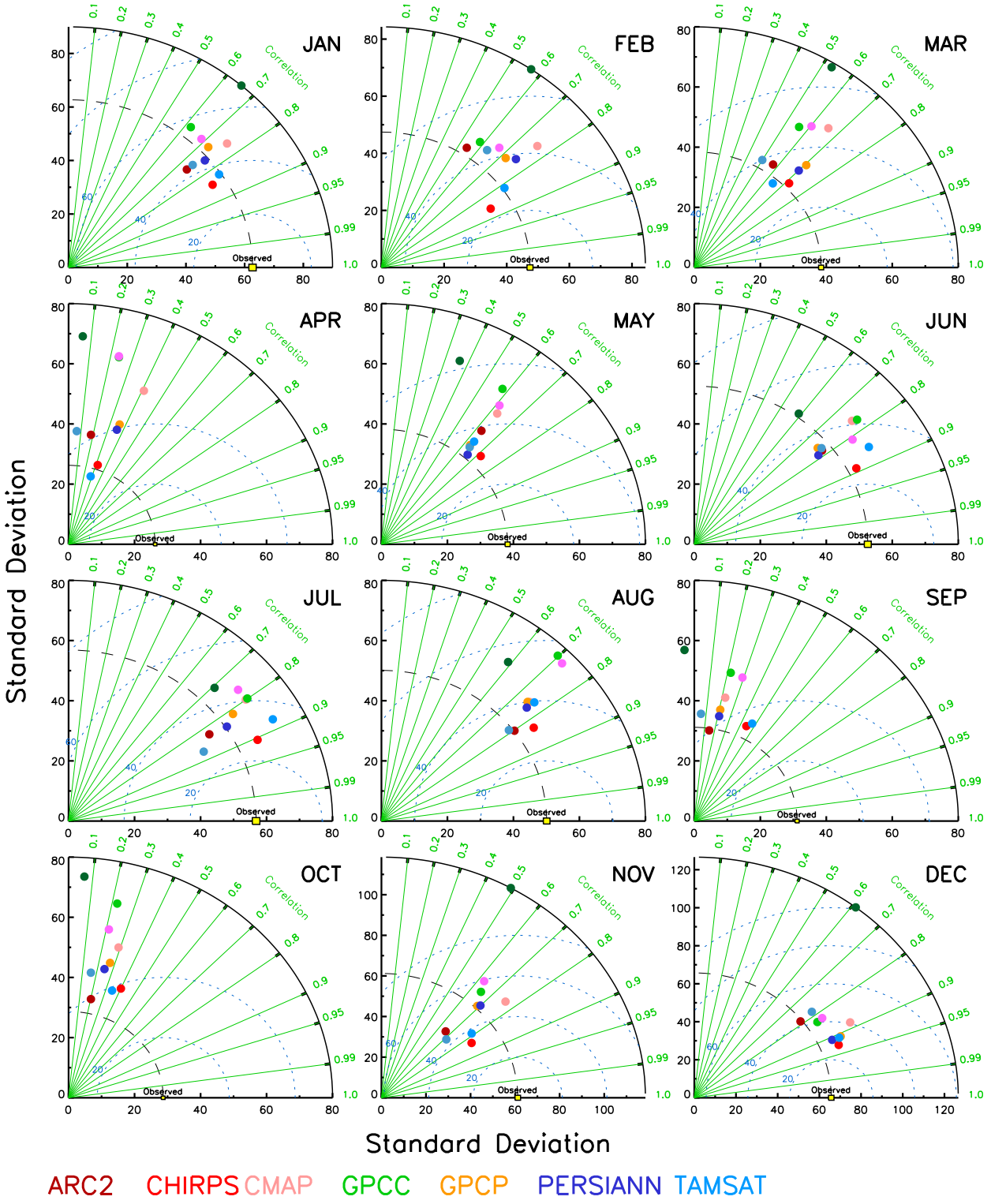

FIG. 8. Taylor diagrams for 1998–2010 for the central basin sector. "Observed" refers to the NIC131 dataset. Analysis uses the "reconstructed" version of NIC131, so that all grid boxes in this sector are included in each month and year. The correlations are based on roughly 206 points. The *x* and *y* axes are standard deviation; the thin green dashed lines are the RMSE.

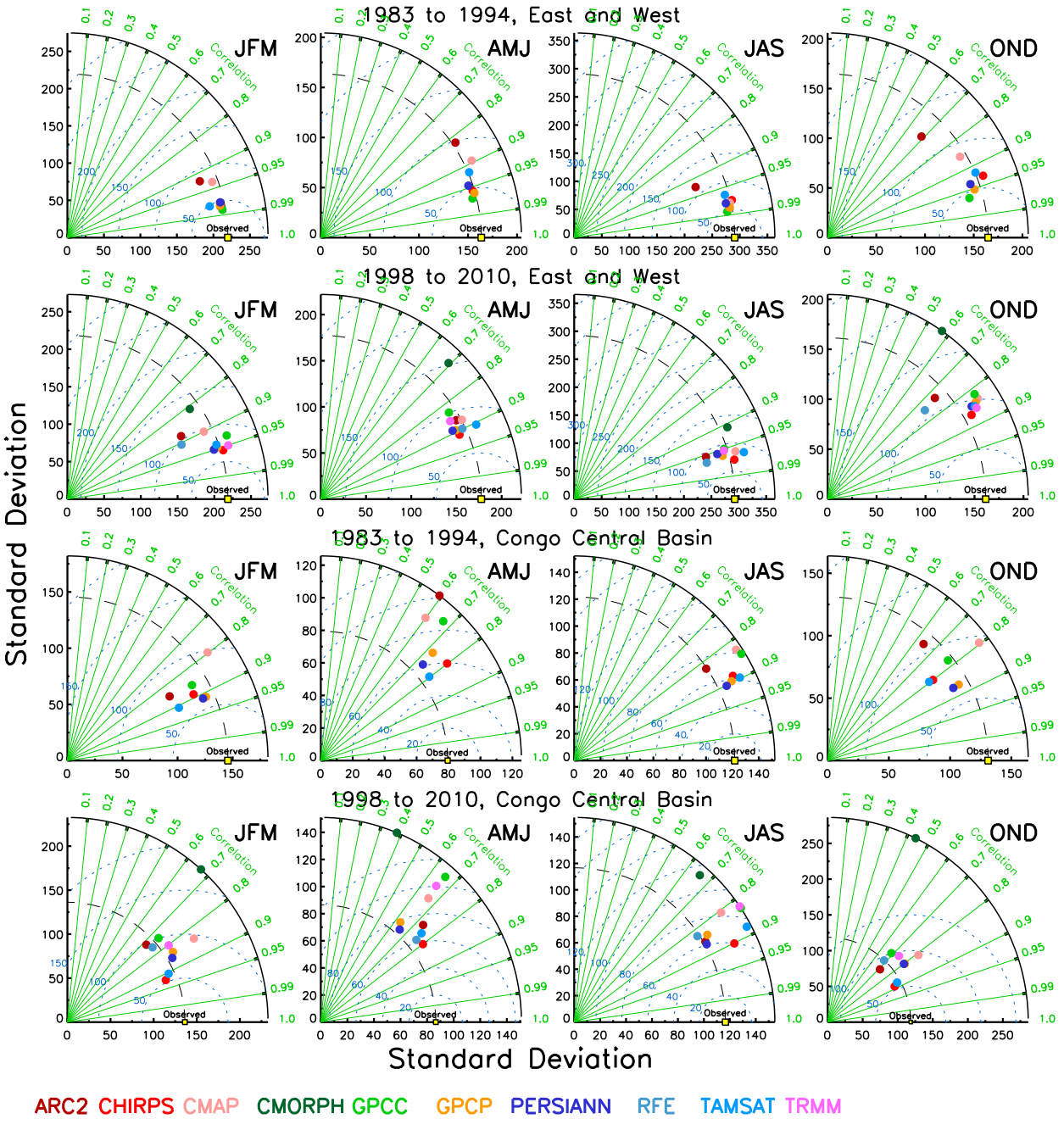

FIG. 9. Taylor diagrams for seasonal rainfall at the two locations and during the two time periods considered.

GPCC V7 also had some of the greatest error in some individual months and seasons.

For the period 1998–2010, when all 10 products are available, the RMSE error, as compared to the NIC131-gridded reference dataset, is considerably greater for all products. Note that the error in the reference dataset is also larger during this period, roughly 10% (Nicholson et al. 2018b). For the east plus west sector CHIRPS2 consistently (10 of 12 cases) has the lowest RMSE during this time period. However, RMSE is only marginally higher for GPCP 2.3, PERSIANN-CDR, and TRMM 3B43. For all four products it is on the order of 30–40 mm for monthly estimates. In contrast to the earlier time period, RMSE is only marginally greater for ARCv2 and TAMSAT V3 than for the other products. The error in TRMM 3B43 and RFE 2.0 is comparable to that for GPCP 2.3 and PERSIANN-CDR. The error in GPCC V7, which has few stations during this time

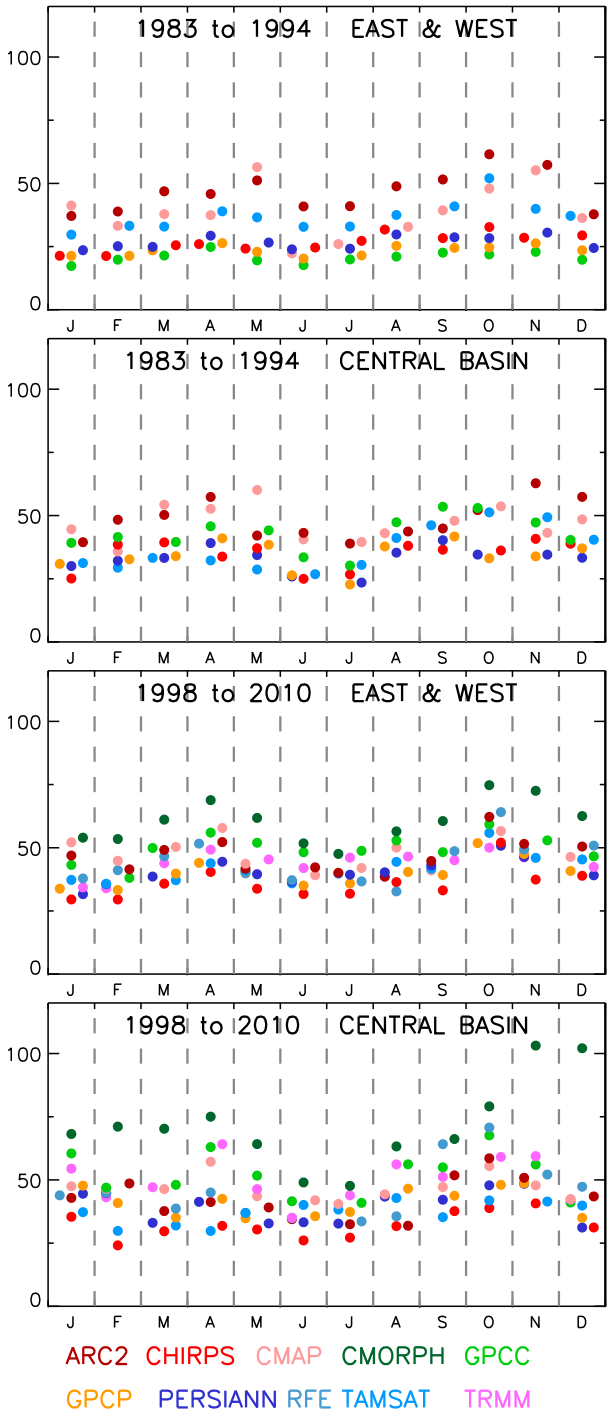

FIG. 10. RMSE (mm month^{-1}) of nine satellite products and GPCC, compared to the reference dataset NIC131, in two sectors and two time periods.

period, is on the order of 40–60 mm for monthly estimates and 85–110 for seasonal estimates. The greatest error is consistently (11 of 12 cases) associated with CMORPH CRT and is on the order of 50–70 mm for monthly estimates.

For the central basin during 1998–2010 RMSE for most of the products is actually slightly lower than for the other sector. The lowest RMSE is again associated with CHIRPS2 (10 of 12 months). TAMSAT V3 and PERSIAN-CDR also have consistently low RMSE. As for the east plus west sector during this time period, CMORPH CRT dramatically overestimates rainfall, compared to the reference dataset and compared to the other rainfall products. Notably, the RMSE in GPCC V7 and TRMM 3B43 also tends to be relatively high, presumably a result of the near absence of GPCC V7 gauge data in this region during 1998–2010.

3) BIAS OF MONTHLY ESTIMATES

The bias of monthly estimates is summarized in Fig. 11. As with RMSE, it is calculated separately for the two time periods and for the east plus west and central basin sectors. During the period 1983–94, the monthly bias for the east plus west sector is generally less than 10 mm, less during the dry months of July–September. For the central basin the bias tends to be larger, but still positive and on the order of 10–15 mm for most products, depending on the month. The products that frequently show notably higher bias in the central basin are ARCv2 and CMAP. Except for those two products, the bias tends to be positive.

The spread of the bias is clearly greater in all months during the period 1998–2010. For the east plus west sector it is still low, generally less than 15 mm. It tends to be negative during January–June and positive for July–December. Only TAMSAT V3 is a consistent outlier, but even so the bias is less than 20 mm. The bias tends to be very low for TRMM 3B43, as also noted by Munzimi et al. (2015), and for both GPCC V7 and GPCP 2.3. For the central basin there is little consistency among the products and months. Occasionally CMAP, RFE 2.0, and ARCv2 are outliers, but in nearly all cases the bias is less than 25 mm.

4) RMSE AND BIAS OF SEASONAL ESTIMATES

Figure 12 shows both RMSE and bias for seasonal estimates. For 1983–94 the RMSE of the best performing products is on the order of 50–60 mm for the east plus west sector and on the order of 60–80 mm in the central basin. Note that this is the error in a 2- or 3-month total and is roughly twice that of the monthly estimates. This suggests that the seasonal aggregation reduces some of the random error in the monthly estimates. ARCv2 is a clear outlier in both cases, with RMSE for the season being as high as 100–120 mm. RMSE is also tends to be high for TAMSAT V3 in the east plus west sector and for CMAP in both sectors. During the period 1998–2010 seasonal RMSE is much greater for both sectors than in the 1983–94 period. It is particularly high for CMORPH CRT, on the order of

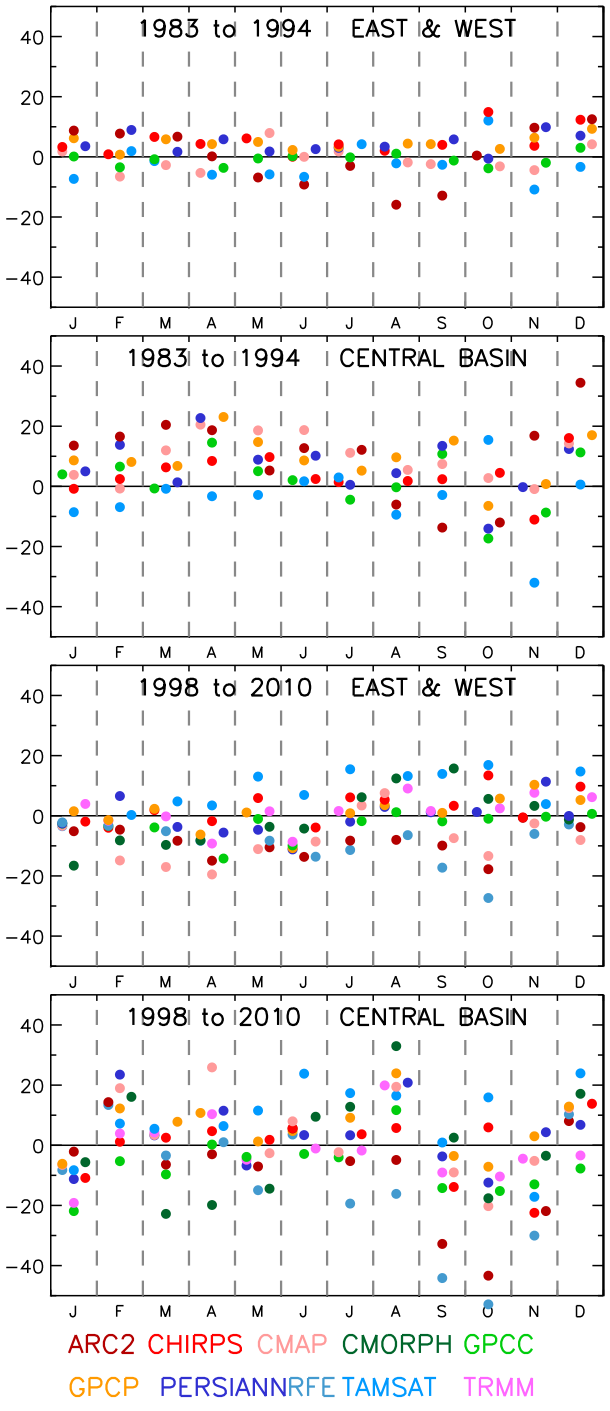

FIG. 11. Bias (mm month^{-1}) of nine satellite products and GPCC, compared to the reference dataset NIC131, in two sectors and time periods.

100–175 mm in both sectors. It is on the order of 60–100 mm for other products and is consistently lowest for CHIRPS2.

The seasonal bias is very low during the period 1983–94 for the east plus west sector. With few exceptions, it is on the order of 10 mm or less and tends to be positive. For the central basin during this period the bias tends to also be positive, but greater, on the order of 20–25 mm in most cases. The exception is AMJ, when the bias ranges from about 10 to 60 mm. Outliers tend to be ARCv2 in the east plus west sector and TAMSAT V3 in the central basin. For the 1998–2010 period there is considerable scatter in the bias of the 10 products, with little tendency to be negative or positive. In most cases it is on the order of 30 mm or less, but the results appear to be random. That is, no product has consistently high or low basis. Again TAMSAT V3 is an exception, having the greatest bias in most seasons during the 1998–2010 period.

b. *Seasonal cycle*

Figure 13 shows the seasonal cycle based on each product and averaged over two locations for the years 1998–2010. The value for the reference dataset, which includes reconstructed values, is shown as a black horizontal line. The locations, shown in the inset, cover most of the Congo basin and are delineated to encompass areas in which the seasonal cycle is relatively homogeneous. One sector spans from the equator to 7.5°N and the other spans from the equator to 7.5°S. The seasonal aggregation is not the standard 3-month periods. Instead, five multimonth periods were selected based on a similar spatial pattern of rainfall during the selected periods. Note that the indicated rainfall is a total for the multimonth period, which can be either two or three months, and not rainfall per month. This format is used, so that the graph also shows the annual total from each product.

The seasonal cycle for the northern region is on the left (Fig. 13). Each of the products except TAMSAT V3 shows excellent agreement with the NIC131-gridded reference dataset (the horizontal black lines on the figure). The seasonal cycle in GPCC V7 is almost identical to that of the reference dataset. August–September (AS) is the wettest season, followed by October–November (ON) and March–April (MA). December–February (DJF) stands out as being very dry. The most anomalous product appears to be TAMSAT V3, which substantially overestimates rainfall in both August–September and May–July (MJJ). Also, ARCv2 and RFE 2.0 overestimate rainfall in the DJF dry season and underestimate rainfall in the AS season. With the exception of TAMSAT V3, the spread of the annual means of the products is about 80 mm, which is about 5% of the annual average of 1559 mm in the reference dataset. In contrast, the annual mean from TAMSAT V3 is 1721 mm, or roughly 15% above the mean for reference dataset.

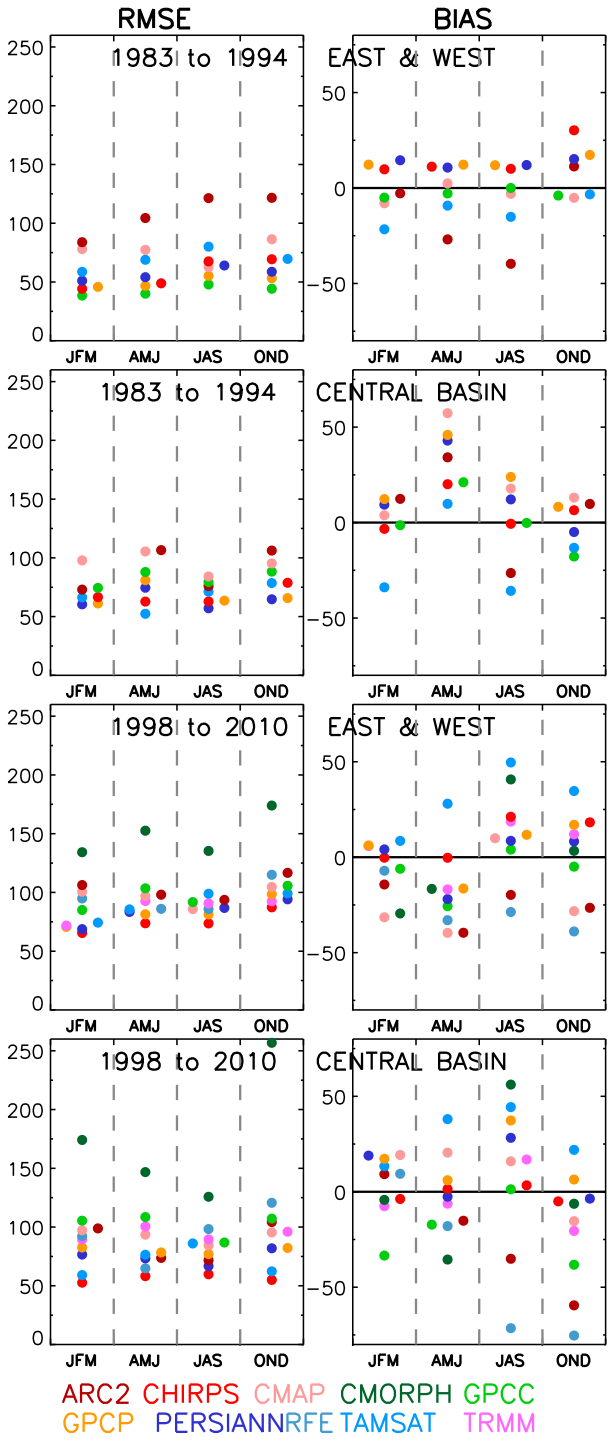

FIG. 12. RMSE and bias of nine satellite products and GPCC in two sectors and time periods on the seasonal scale.

The situation is very different in the southern region, on the right of the diagram (Fig. 13). All of the products show essentially the same seasonal cycle. The DJF, ON, and MA seasons are almost equally wet (in terms of mm month^{-1}), while MJJ and AS are clearly very dry. However, a fair amount of scatter is apparent among the 10 products. This occurs primarily during October–November, but is apparent in other seasons as well. The spread of the annual means among the products is over 250 mm. RFE 2.0 is the lowest, at 1461 mm, and GPCP 2.3 is the highest, at 1713 mm. The reference mean is 1560 mm. An unexpected result is that the spread between GPCC V7 and GPCP 2.3, which is very dependent on GPCC, is 226 mm. TRMM 3B43 and CHIRPS2 show a seasonal cycle that is extremely similar to that of the reference dataset. CMAP is also fairly similar, despite the poor performance of CMAP that was suggested by other analyses in our study.

c. *Meridional transects*

The spatial integrity of the estimates is examined using two meridional transects (Fig. 14), one in the western Congo basin at 20°E and one in the eastern Congo at 30°E. The plotted values represent a 5° longitudinal span, that is, one 2.5° grid box on either side of the indicated longitude. Values of rainfall along the transects are shown for two different time periods and for each season. The first period is 1983–94, when the station network was quite dense; NIC131-gridded values are estimated via spatial reconstruction at only a few grid points. The second is 1998–2010, when most of the NIC131-gridded reference values are reconstructed. Only seven products are available in the first period, but all 10 are available in the second.

Along the western transect for the period 1983–94 there is excellent agreement among most satellite products and these agree exceedingly well with the NIC131-gridded gauge dataset and with GPCC V7. All show a shift of the rainfall maximum from roughly 10°N in JAS to 10°S in JFM. The only clear outliers are the lower values of ARCv2 in JAS in northern latitudes and the southward displaced maxima in CMAP in AMJ and in CMAP and ARCv2 in OND. In 1998–2010 the spread of the estimates is much greater in all seasons except JJA, but most products show reasonable agreement with the NIC131-gridded gauge data. The exception is CMORPH CRT, which shows anomalously low values in three of the four seasons. ARCv2 and RFE 2.0 are also very low in JFM and OND.

At 30°E, similar conclusions can be drawn. There is generally excellent agreement among satellite products, GPCC V7, and the NIC131-gridded dataset for 1983–94. As at 20°E, ARCv2 is an outlier, being generally higher than other estimates in MAM and SON, but notably lower in most of the southern latitudes in DJF (which is the rainy season in the south). In OND disparities are apparent with respect to the latitude of maximum rainfall, with some products even showing a double

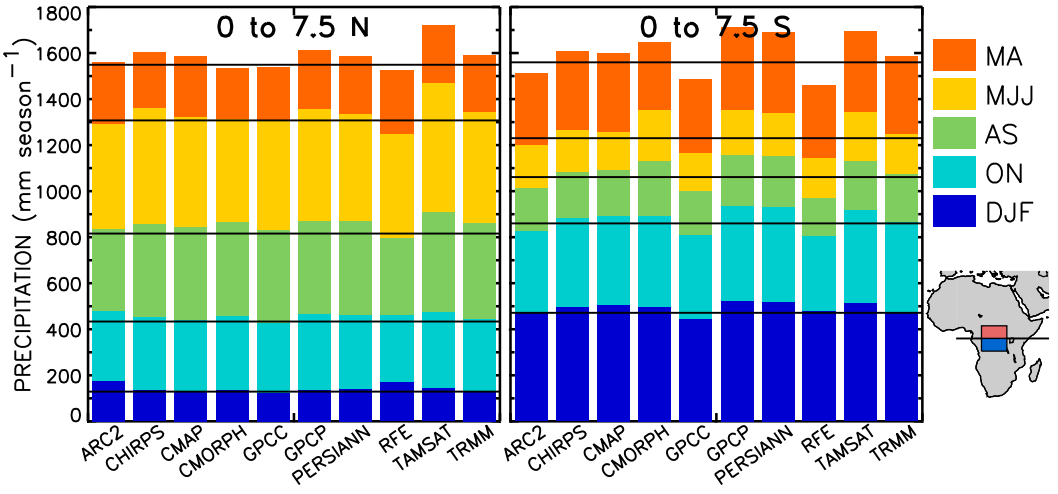

FIG. 13. Seasonal cycle with inset showing two box locations over which the seasonal cycle is calculated. (left) The northern box and (right) the southern box. Black horizontal lines indicate the mean for the season in the NIC131 reference dataset. Data are for the years 1998–2010, so that all products could be included.

maximum. All, however, show a broad area of maximum rainfall from roughly 5°N to 10°S. As at 20°E, the spread of the estimates is much larger for 1998–2010 than for 1983–94. CMORPH CRT is shown to have the most extreme values and is a strong outlier near the equator in MAM and SON. The spread among the estimates is particularly large for the rainfall maxima in JFM and JAS, when the rain belt reaches its southern and northern extremes.

d. Interannual variability

To compare the performance of the various products in capturing interannual variability, four regions were selected (Fig. 1) based on the availability of gauge data and on the spatial coherence of rainfall. Two are in the western Congo basin, one is the northern Congo basin, and one is the eastern Congo basin. To facilitate the discussion, the regions are termed Gabon, DRC, Central African Republic (CAR), and Uganda. To examine variability within the heart of the basin, a fifth region was selected, even though few stations are available during the period 1989–2010. It is termed Congo basin and is close to the sector termed ''central basin'' in prior analyses. Calculations are done for the MA and ON seasons, the rainiest periods for equatorial Africa. In this case, only six products plus the NIC131-gridded reference data are shown. ARCv2, RFE 2.0, CMAP, and CMORPH CRT are omitted because they are not continuous over this time period and because each these products was frequently a strong outlier in other analyses.

Figure 15 shows the time series for each region from 1983 to 2010 and the number of stations available in the region in each year. The time series represent a simple average of the 2.5° grid boxes in each region, four in the cases of Gabon, DRC, and Uganda, six for the Congo basin, and eight for CAR (Fig. 1). The total number of stations in NIC131 and in GPCC V7 in each year is indicated at the bottom of the diagrams.

Table 2 summarizes the correlation of each time series with that of NIC131-gridded. The correlations suggest that there is generally good agreement among the various datasets. The exceptions are for the Congo basin and, to a lesser extent, DRC. Correlations, based generally on 28 years, tend to range from 0.5 to 0.9. However, for the Congo basin in October–November they range from −0.004 to 0.33. For DRC for the same season they range from 0.20 to 0.53. For both locations they are considerably higher during March–April (TRMM 3B43 is an exception). Note also that the highest correlations tend to be with CHIRPS2, especially in these two data-sparse regions.

The time series in Fig. 15 show the relationships with more detail. Again, except in the Congo basin, there is reasonable agreement among most of the products. Some tend to overestimate rainfall in the Gabon sector and during ON in the CAR sector, as compared to the NIC131 reference dataset. The scatter of the estimates becomes noticeably greater after the mid-1990s, when gauge data become much more scarce. All products appear to capture the shift from an ON maximum in the west to a MA maximum in the east. In most cases there tends to be more scatter in ON than in MA.

There is little scatter among the estimates for the CAR region. However, a noticeable disparity occurs in ON in 1997. NIC131-gridded and CHIRPS2 both

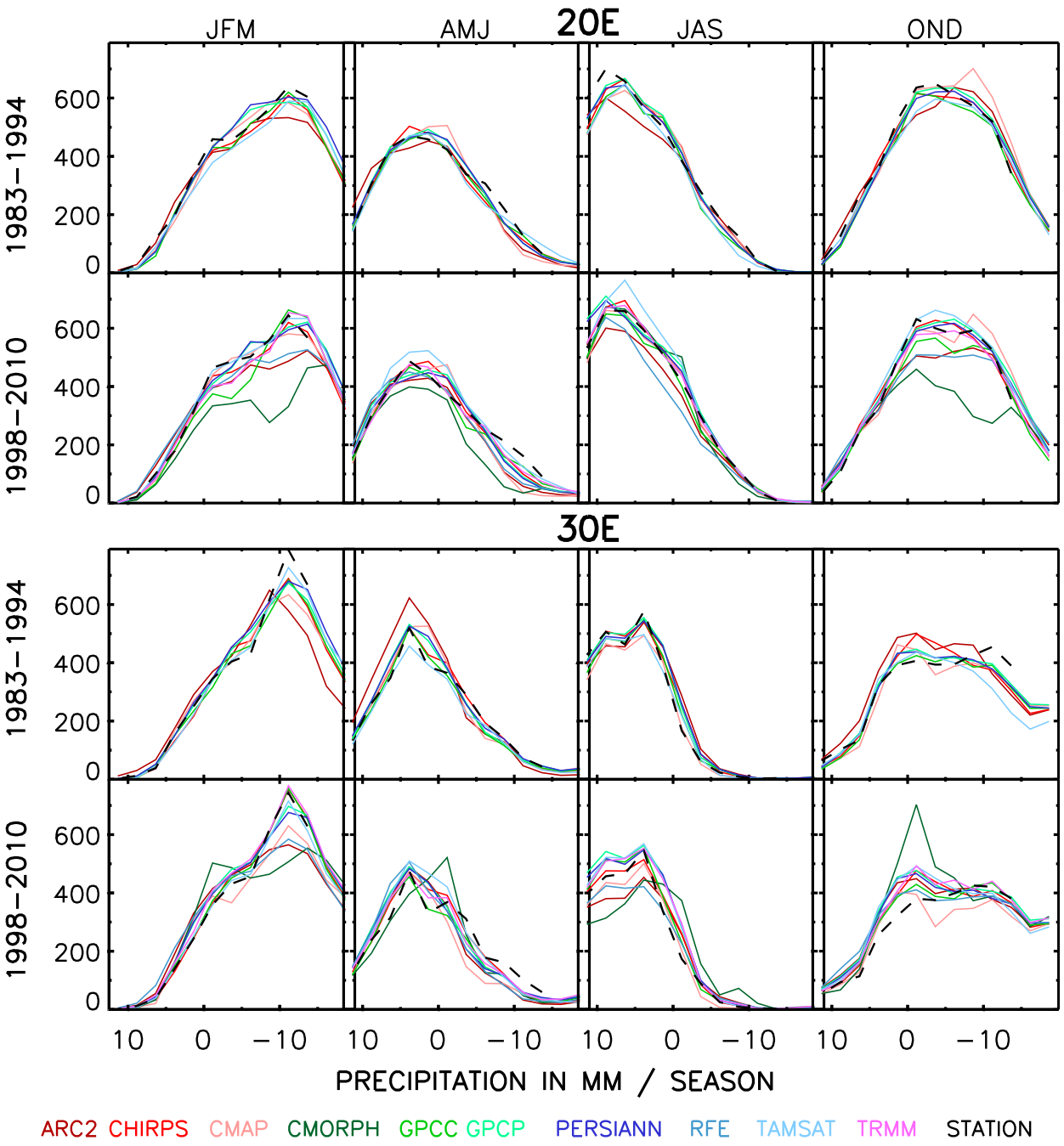

FIG. 14. Meridional transects of seasonal rainfall (mm month^{-1}) for both time periods: (top) 20°E and (bottom) 30°E. Precipitation (y axis) is given in millimeters per season.

indicate roughly 325 mm, while the remaining products cluster around 150 mm. The agreement among those products likely reflects the influence of GPCC V7 on the two satellite estimates. It is not readily apparent which values are correct. However, ON of 1997 tends to be wet in each of the nearby regions, suggesting that the higher values are correct. It can also be argued that the values are so low in that year in the CAR region and also in DRC that they are somewhat unrealistic.

The scatter among the estimates is also relatively small for the Uganda sector. This is an area of high station density in both NIC131 and GPCC V7. Although the number of stations decreased in 2001, a large change in the scatter among the estimates did not occur.

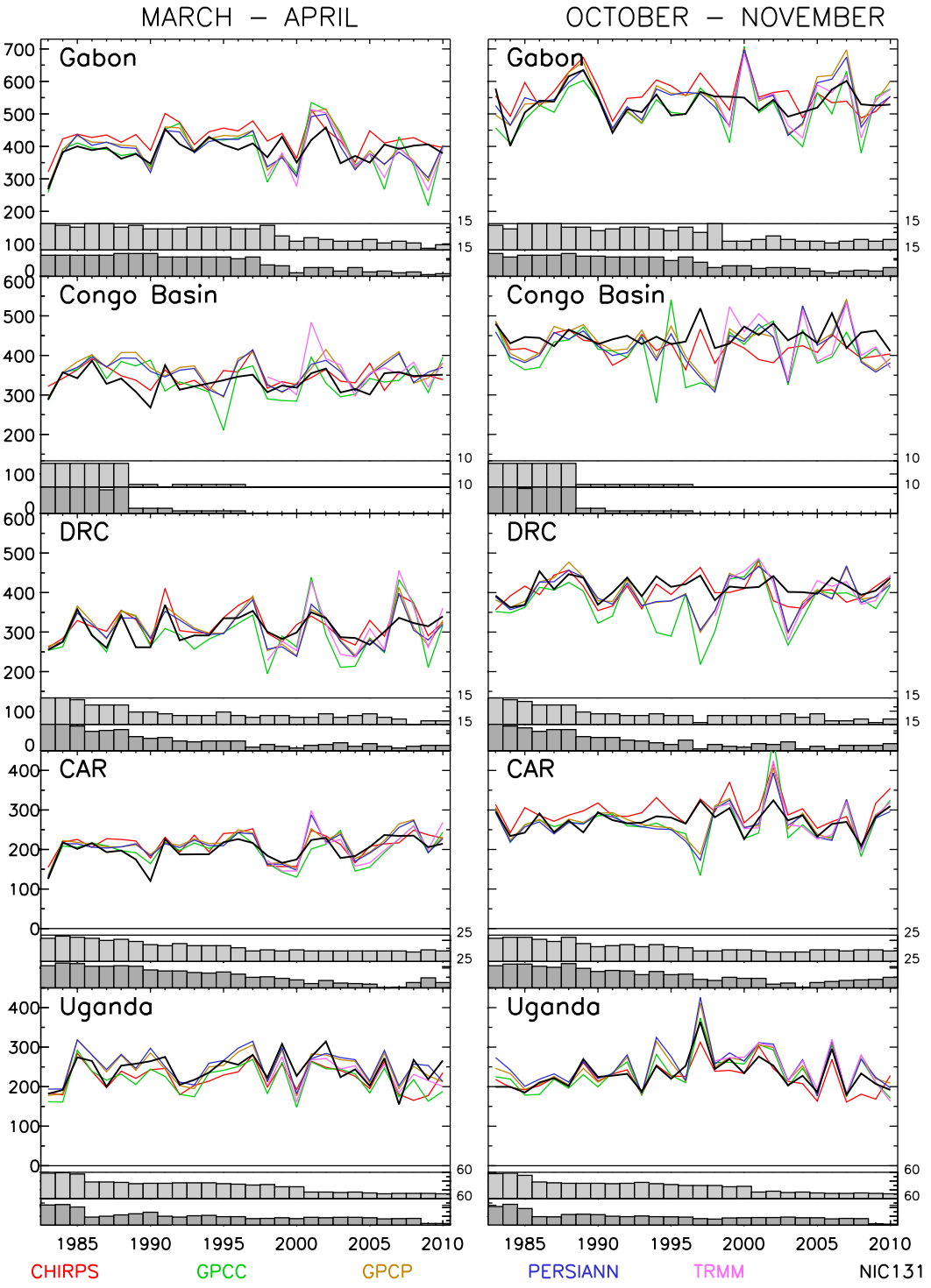

FIG. 15. Interannual variability (mm yr^{-1}) in Gabon, Congo, DRC, CAR, and Uganda (see Fig. 1 for location). The numbers of stations for NIC131 and GPCC are shown as the rows of light and darker gray boxes, respectively.

For the westernmost sector, termed Gabon, an increase in scatter is readily apparent when the number of stations greatly decreases in the late 1990s. Notable is the year 2000, when most products show a very wet year, but NIC131-gridded shows a relatively dry year. NIC131-gridded also suggests that relatively dry conditions occurred after 1998, but this could reflect the dramatic reduction in station number after 1998. After that

TABLE 2. Correlation of the time series in Fig. 15 with the NIC131-gridded dataset.

Season	Area	Source				
		CHIRPS2	GPCC	GPCP	PERSIANN	TRMM
MA	Gabon	0.74	0.52	0.68	0.67	0.43
MA	Congo basin	0.52	0.26	0.39	0.43	0.46
MA	DRC	0.74	0.56	0.64	0.65	0.73
MA	CAR	0.71	0.65	0.72	0.69	0.66
MA	Uganda	0.76	0.74	0.77	0.74	0.73
ON	Gabon	0.54	0.55	0.64	0.62	0.50
ON	Congo basin	0.33	0.03	−0.02	−0.004	0.14
ON	DRC	0.46	0.20	0.38	0.39	0.53
ON	CAR	0.83	0.47	0.53	0.49	0.82
ON	Uganda	0.85	0.89	0.89	0.88	0.93

time, the records from the country of Gabon became unavailable and the remaining stations are all in the Congo, a somewhat drier region.

For both the region termed DRC and the region termed Congo basin the scatter among the estimates becomes notably greater since the late 1990s. This is especially true for ON estimates. Particularly troubling is the divergence between the estimates of NIC131-gridded and GPCC V7 in these regions since the early 1990s. Both are gauge-only products but different methods are used to fill in the considerable gaps in these regions.

This disparity and other results of this analysis clearly demonstrate the impact of decreasing station number. This impact is also evident in the contrast in the agreement of the various products between the data-poor Congo basin and DRC versus the data-rich regions of Gabon, CAR, and Uganda. It is equally clear from the increase in the scatter of the products as the station numbers decrease following the 1980s or 1990s.

6. Summary and conclusions

In this study satellite rainfall estimates and GPCC V7 are evaluated by comparison with a dense gauge dataset newly developed for equatorial Africa. For error calculations two geographical areas and two time periods are considered. One sector (east plus west) combines two geographical regions on the eastern and western periphery of the Congo basin. The second sector is in the central basin of the Congo. The time periods are 1983–94 and 1998–2010, respectively. In the east plus west sector, gauge data are relatively plentiful in both periods. In the central basin, gauge data are scarce during the earlier period and almost totally lacking in the second.

For the period 1983–94, during which seven of the evaluated products are available, the network is dense enough that complete confidence can be placed on the NIC131-gridded reference dataset. For the period 1998–2010 few gauge data are available in the central Congo basin and most of the gridded rainfall estimates of NIC131 are based on a statistical reconstruction method that extrapolates from the stations around the periphery of the basin. Hence, it cannot be assumed a priori that discrepancies between that and the other rainfall products necessarily reflect error in the other products. Nevertheless, the argument can be made that NIC131-gridded provides the best rainfall estimates over the Congo during the 1998–2010 period. For one, that dataset has been validated and shown to have an RMSE of roughly 10%. Second, the large spread of the satellite estimates during that period reduces the confidence in those estimates. Finally, NIC131-gridded generally agrees closely with CHIRPS2, the only product other than TAMSATV3 that has no dependence on GPCC.

The performance of the various satellite products varies to some extent between the two time periods and two locations considered. During the period 1983–94, GPCC V7 has the lowest RMSE, near zero bias, and some of the highest correlations with NIC131-gridded rainfall data for the eastern and western peripheries of the basin. This is not surprising, since both include an almost identical set of stations during this time period. The performance of GPCP 2.3, PERSIANN-CDR, and CHIRPS2 is only marginally weaker than that of GPCC V7. The products with the greatest error are ARCv2 and CMAP. For the central basin during this time period, none of the products is consistently the best. However, CHIRPS2, TAMSAT V3, PERSIANN-CDR, and GPCC V7 have consistently low RMSE, and the RMSE of both ARCv2 and CMAP is generally among the largest. In terms of correlation with the reference dataset, the highest is generally with CHIRPS2, GPCP 2.3, and PERSIAN CDR. The bias is generally low, but roughly twice as great as with the east plus west sector, and it tends to be positive. Note that the correlations are consistently lower for the central basin than for the east plus west periphery.

During the period 1998–2010 what clearly stands out is the increased scatter in the error estimates of the various products, the lower correlation with NIC131-gridded, and the higher RMSE and bias compared to NIC131-gridded. This is much less of a problem for the east plus west sector, where there are adequate stations in the NIC131 reference dataset, than for the data-sparse central basin. Although the correlations are lower and the RMSE error is higher than for the previous period, for the east plus west sector they still tend to be on the order of 0.7–0.9 for most products in all months but April. The best agreement with NIC131-gridded is CHIRPS2; the standard deviation is the same in both and the correlation between them is generally between 0.8 and 0.9, and the RMSE for CHIRPS2 is consistently the lowest among the products. The RMSE is only marginally greater for GPCP 2.3, PERSIANN-CDR, and TRMM 3B43. In contrast, ARCv2, RFE 2.0, CMAP, and CMORPH CRT are frequent outliers. The performance of satellite products in comparison to NIC131-gridded is notably poorer for the central basin. Once again, there is fairly strong and consistent agreement between NIC131-gridded and CHIRPS2 and CMORPH CRT is consistently an outlier.

One perplexing result is the weak correlation of all products with the reference dataset in the wettest months, particularly April. This is seen in three of the four cases considered but is not apparent in the bias or RMSE. We hypothesize that the low correlations are related to the relative uniformity of rainfall in the analysis sector in the wettest months. Figure 16 provides evidence of this, using the central basin sector as an example. The correlation between the standard deviation of the observations (i.e., of the NIC131-gridded reference dataset) within the sector and the average of correlation of the 10 products with the observations is 0.9. In April, September, and October, the standard deviation is on the order of 25–30 mm and the average correlation is around 0.25. For the other months, the standard deviation ranges from about 35 to 75 mm, and the average correlations range from around 0.6 to 0.9.

A possible interpretation is that in the wet months of April, September, and October the error in the individual products (and in the reference dataset) is relatively large compared to the scatter of the observations within the analysis sector. In the absence of a dense station network to ''anchor'' the various products, relatively small spatial variations cannot be captured. Support for this interpretation is that when the correlation is lower, the density of observations is lower. Thus, the correlations are not anomalously low in the wet months for the east plus west sector during the 1983–94 period. In the east plus west for the 1983–94 period, when the station density is still relatively dense, the correlations with the reference dataset are around 0.6–0.8. They fall to 0.3–0.5 for the central basin in 1983–94 and to 0.1–0.4 for the central basin in 1998–2010, when there is almost a complete absence of station data.

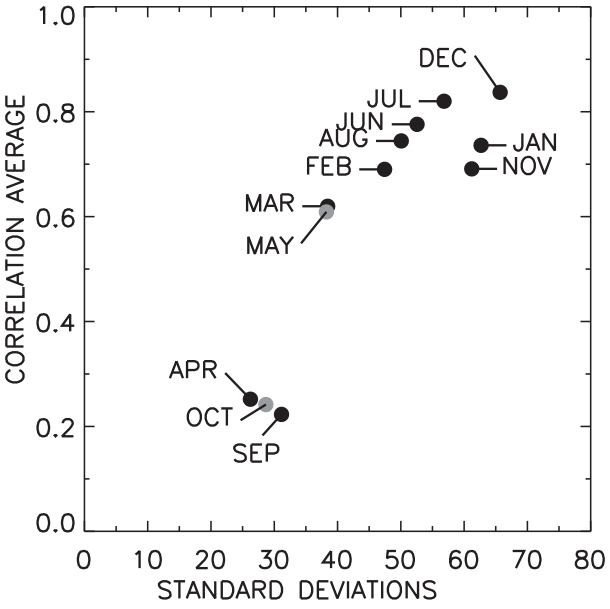

FIG. 16. Comparison of standard deviation of monthly values in the reference dataset with the average correlation of the reference dataset with the nine satellite products plus GPCC for the period 1998–2010. Data are for the central basin sector.

Another finding is that, in general, temporal or spatial averaging tends to reduce the error in the estimates. One example is the relative error in the seasonal estimates, which (calculated per month) is lower than for the individual months. Similarly, all products tend to adequately produce the mean seasonal cycle even in the more central regions of the Congo basin. However, north of the equator, TAMSAT V3, ARCv2, and RFE 2.0 tend to over or underestimate rainfall in some seasons. Annual means of the various products, with the exception of TAMSAT V3, vary by roughly 5%. South of the equator there is more scatter among the products in the estimation of seasonal rainfall, especially during the October–November season. There annual means vary by 250 mm, which is roughly 15% of the reference mean. Notably, the station network is denser in the more northern sector. The mean meridional transects also show fairly close agreement among most products. This includes not only the magnitude of rainfall along the transect, but also the seasonal changes in the magnitude of rainfall and the location of the rainfall maxima. However, the products that generally perform poorly in other cases stand out here as outliers as well: CMORPH CRT, ARCv2, and CMAP.

There is a wide range of disparity in the rainfall estimates of the 10 products. Several products are consistently shown as outliers in each of the analyses and should not be used in climatological studies for the Congo basin. These include ARCv2, CMORPH CRT, and CMAP. RFE 2.0 and TAMSAT V3 are also frequent outliers. Notably, TAMSAT V3 appears to be in general unreliable in recent decades, even though it is only calibrated with historical gauge data and is not merged with gauge data. Our results suggest that the remaining products all perform relatively well in this region. All appear to provide generally good monthly estimates of rainfall throughout the region and can readily reproduce the seasonal cycle and the meridional variations of rainfall. However, CHIRPS2 tends to show the greatest relationship to the NIC131-gridded reference dataset in almost all cases, and it particularly stands out as probably the best monthly satellite product to use in recent years in the central Congo basin.

The contrasts in the algorithms utilized to incorporate gauge data in the various satellite products may explain the diversity in performance. The contrasts are 1) whether the product is merged with or adjusted by gauge data, 2) which gauge set is used, and 3) the interpolation techniques. Points two and three may be the pivotal differences. Most of the products utilize GTS or GPCC data. The GTS data for the Congo basin region are extremely sparse and erratically available. GPCC, while including GTS, also receives data directly from the African meteorological services. GPCP 2.3, TRMM V7, and PERSIANN-CDR all rely on GPCC gauge data, hence have generally similar performance. TAMSAT only uses historical estimates, which has the advantage of a large database, but these estimates are not contemporaneous with the satellite products. Via agreement with agencies within Africa, CHIRPS has access to a variety of gauge datasets not incorporated into the other products. A more substantial difference may be the technique of spatial interpolation used to fill in the huge gaps in the Congo basin. Where large gaps in the station network exist, none of the standard approaches to gridding is very reliable (Long et al. 2016), especially in data-sparse locations such as the Congo basin. CHIRPS, which is arguably the best performing product, instead takes the spatial correlation structure into account.

Collectively, our results suggest that there is considerable uncertainty in any of the rainfall products over the most central sector of the Congo basin during the period 1998–2010. These uncertainties must be taken into account in evaluating rainfall variability in this region. The problem of discrepancies here and elsewhere in central equatorial Africa has been noted by others, such as Negron Juarez et al. (2009), Sun et al. (2018), and Beighley et al. (2011). Based on comparison with streamflow and water storages, Beighley et al. (2011) found that TRMM 3B42 provides better rainfall estimates than CMORPH CRT or PERSIANN-CDR over the Congo River basin as a whole. They did conclude that all three satellite products provide unreasonably high values in some periods: all three in ON and CMORPH CRT and PERSIANN-CDR in MA. They concluded that all three products tended to overestimate rainfall magnitude, especially in the central basin. In contrast our results suggest that the TRMM tends to underestimate rainfall in this region. Beighley et al. (2011) calculated that annual rainfall was on the order of 1200–1600 mm in most of the Congo basin. Our results here suggest that 1600 mm yr^{-1} is more likely for this region. Munzimi et al. (2015) also found that TRMM 3B42 underestimates rainfall over the Congo.

Munzimi et al. (2015) used the few available gauge stations to adjust TRMM 3B42 in this region. Based on a comparison with historical gauge data, they concluded that the TRMM 3B43 product and their TRMM3B42-adjusted product performed relatively well over the Congo basin. Our results are less optimistic about the performance of TRMM 3B43 and other products in the region. Their conclusion was based on long-term means and assessed the ability to capture the mean spatial pattern of variability in the region. Our results likewise showed that several products could capture the mean spatial pattern, but also showed that individual monthly estimates and estimates of interannual variability are much less reliable.

One of the most important points that emerges from this study is the importance of having at least a few gauge stations for merging with or calibrating the satellite product. This is clearly shown by the large increase in scatter in the 1990s, when the station count rapidly decreases. A similar conclusion was reached by Yin et al. (2004) in evaluating the performance of GPCP 2.3 and CMAP in this region. Efforts are being made to increase the number of weather stations across the continent (van de Giesen et al. 2014; Dezfuli et al. 2017). Until that is done, the best approach to examining interannual variability may be an integrated one, considering for example, various hydrologic parameters obtainable from space (e.g., Beighley et al. 2011). The approach of Munzimi et al. (2015) in adjusting products with the available gauge data is also a good one. Increased availability of gauge data would make that approach even more promising. The situation can also be improved by increasing the collaborative relationships with the African meteorological services. Adding the availability of station data in a few key areas can also

make a large difference in the reliability of satellite estimates of African rainfall.

Acknowledgments. The project was supported by the National Science Foundation (NSF AGS-1535426 and AGS-1535439). We would also like to acknowledge the sources of data used in the manuscript. ARCv2 and RFE 2.0 data were obtained from the NOAA National Centers for Environmental Information. CMAP, GPCP 2.3, and GPCC V7 data were provided by the NOAA/OAR/ESRL PSD, Boulder, Colorado, from their website at https://www.esrl.noaa.gov/psd/. PERSIANN data were created by Sorooshian et al. (2014). The TRMM precipitation data were provided by the NASA/Goddard Space Flight Center and PPS, which develop and compute the data as a contribution to TRMM, and archived at the NASA GES DISC. We also greatly appreciate the efforts of the Climate Hazards Group of the University of California, Santa Barbara, and the TAMSAT group at the University of Reading in creating and providing the CHIRPS2 and TAMSAT data, respectively. Finally, we appreciate the efforts of the Research Data Archive at the National Center for Atmospheric Research, Computational and Information Systems Laboratory for providing the CMORPH CRT dataset on their web site (https://doi.org/10.5065/D6CZ356W).

REFERENCES

Adler, R. F., and Coauthors, 2003: The version 2 Global Precipitation Climatology Project (GPCP) monthly precipitation analysis (1979–present). *J. Hydrometeor.*, **4**, 1147–1167, https://doi.org/10.1175/1525-7541(2003)004<1147:TVGPCP>2.0.CO;2.

Asadullah, A., N. McIntyre, and M. Kigobe, 2008: Evaluation of five satellite products for estimation of rainfall over Uganda. *Hydrol. Sci. J.*, **53**, 1137–1150, https://doi.org/10.1623/hysj.53.6.1137.

Ashouri, H., K. L. Hsu, S. Sorooshian, D. K. Braithwaite, K. R. Knapp, L. D. Cecil, B. R. Nelson, and O. P. Prat, 2015: PERSIANN-CDR: Daily precipitation climate data record from multisatellite observations for hydrological and climate studies. *Bull. Amer. Meteor. Soc.*, **96**, 69–83, https://doi.org/10.1175/BAMS-D-13-00068.1.

Awange, J. L., V. G. Ferreira, E. Forootan, Khandu, S. A. Andam-Akorful, N. O. Agutu, and X. F. He, 2016: Uncertainties in remotely sensed precipitation data over Africa. *Int. J. Climatol.*, **36**, 303–323, https://doi.org/10.1002/joc.4346.

Balas, N., S. E. Nicholson, and D. Klotter, 2007: The relationship of rainfall variability in west central Africa to sea-surface temperature fluctuations. *Int. J. Climatol.*, **27**, 1335–1349, https://doi.org/10.1002/joc.1456.

Beighley, R. E., and Coauthors, 2011: Comparing satellite derived precipitation datasets using the Hillslope River Routing (HRR) model in the Congo River Basin. *Hydrol. Processes*, **25**, 3216–3229, https://doi.org/10.1002/hyp.8045.

Berhane, F., B. Zaitchik, and H. S. Badr, 2015: The Madden–Julian oscillation's influence on spring rainy season precipitation over equatorial West Africa. *J. Climate*, **28**, 8653–8672, https://doi.org/10.1175/JCLI-D-14-00510.1.

Cattani, E., A. Merino, and V. Levizzani, 2016: Evaluation of monthly satellite-derived precipitation products over East Africa. *J. Hydrometeor.*, **17**, 2555–2573, https://doi.org/10.1175/JHM-D-15-0042.1.

Cook, K. H., and E. K. Vizy, 2016: The Congo Basin Walker circulation: Dynamics and connections to precipitation. *Climate Dyn.*, **47**, 697–717, https://doi.org/10.1007/s00382-015-2864-y.

Dezfuli, A. K., 2011: Spatio-temporal variability of seasonal rainfall in western equatorial Africa. *Theor. Appl. Climatol.*, **104**, 57–69, https://doi.org/10.1007/s00704-010-0321-8.

——, and S. E. Nicholson, 2013: The relationship of interannual variability in western equatorial Africa to the tropical oceans and atmospheric circulation. Part II. The boreal autumn. *J. Climate*, **26**, 66–84, https://doi.org/10.1175/JCLI-D-11-00686.1.

——, B. F. Zaitchik, and A. Gnadadesikan, 2015: Regional atmospheric circulation and rainfall variability in south equatorial Africa. *J. Climate*, **28**, 809–818, https://doi.org/10.1175/JCLI-D-14-00333.1.

——, and Coauthors, 2017: Validation of IMERG precipitation in Africa. *J. Hydrometeor.*, **18**, 2817–2825, https://doi.org/10.1175/JHM-D-17-0139.1.

Diem, J. E., J. Hartler, and S. J. Ryan, 2014: Validation of satellite rainfall products for western Uganda. *J. Hydrometeor.*, **15**, 2030–2036, https://doi.org/10.1175/JHM-D-13-0193.1.

Dinku, T., P. Ceccato, E. Grover-Kopec, M. Lemma, S. J. Connor, and C. F. Ropelewski, 2007: Validation of satellite rainfall products over East Africa's complex topography. *Int. J. Remote Sens.*, **28**, 1503–1526, https://doi.org/10.1080/01431160600954688.

——, ——, and S. J. Connor, 2011a: Challenges of satellite rainfall estimation over mountainous and arid parts of east Africa. *Int. J. Remote Sens.*, **32**, 5965–5979, https://doi.org/10.1080/01431161.2010.499381.

——, S. J. Connor, and P. Ceccato, 2011b: Evaluation of satellite rainfall estimates and gridded gauge products over the Upper Blue Nile region. *Nile River Basin: Hydrology, Climate and Water Use*, A. M. Melesse, Ed., Springer, 109–127, https://doi.org/10.1007/978-94-007-0689-7_5.

——, K. Hailemariam, R. Maidment, E. Tarnavsky, and S. Connor, 2014: Combined use of satellite estimates and rain gauge observations to generate high-quality historical rainfall time series over Ethiopia. *Int. J. Climatol.*, **34**, 2489–2504, https://doi.org/10.1002/joc.3855.

Dyer, E. L. E., D. B. Jonex, J. Nusbaumer, H. Li, O. Collilh, G. Vettoretti, and D. Noone, 2017: Congo Basin precipitation: Assessing seasonality, regional interactions, and sources of moisture. *J. Geophys. Res. Atmos.*, **122**, 6882–6898, https://doi.org/10.1002/2016JD026240.

Funk, C., and Coauthors, 2015: The climate hazards infrared precipitation with stations – A new environmental record for monitoring extremes. *Sci. Data*, **2**, 150066, https://doi.org/10.1038/sdata.2015.66.

Gebremichael, J., M. M. Bitew, F. A. Hirpa, and G. N. Tesfay, 2014: Accuracy of satellite rainfall estimates in the Blue Nile Basin: Lowland plain versus highland mountain. *Water Resour. Res.*, **50**, 8775–8790, https://doi.org/10.1002/2013WR014500.

Gu, G. J., 2009: Intraseasonal variability in the equatorial Atlantic-West Africa during March–June. *Climate Dyn.*, **32**, 457–471, https://doi.org/10.1007/s00382-008-0428-0.

Haile, A. T., E. Habib, M. Elsaadani, and T. Rientjes, 2013: Inter-comparison of satellite rainfall products for representing rainfall diurnal cycle over the Nile basin.

Int. J. Appl. Earth Obs., **21**, 230–240, https://doi.org/10.1016/j.jag.2012.08.012.

Hirst, A. C., and S. Hastenrath, 1983: Diagnostics of hydrometeorological anomalies in the Zaire (Congo) basin. *Quart. J. Roy. Meteor. Soc.*, **109**, 881–892, https://doi.org/10.1002/qj.49710946213.

Hoell, A., and C. Funk, 2013: The ENSO-related West Pacific Sea surface temperature gradient. *J. Climate*, **26**, 9545–9562, https://doi.org/10.1175/JCLI-D-12-00344.1.

Hua, W., L. Zhou, H. Chen, S. E. Nicholson, R. Raghavendra, and Y. Jian, 2016: Possible causes of central equatorial long-term drought. *Environ. Res. Lett.*, **11**, 124002, https://doi.org/10.1088/1748-9326/11/12/124002.

——, ——, ——, ——, Y. Jiang, and R. Raghavendra, 2018: Understanding the central equatorial Africa long-term drought using AMIP-type simulations. *Climate Dyn.*, **50**, 1115–1128, https://doi.org/10.1007/s00382-017-3665-2.

Huffman, G. J., and D. T. Bolvin, 2014: TRMM and other data precipitation data set documentation. NASA TRMM Doc., 42 pp., ftp://precip.gsfc.nasa.gov/pub/trmmdocs/3B42_3B43_doc.pdf.

——, and Coauthors, 2007: The TRMM Multi-satellite precipitation analysis: Quasi-global, multi-year, combined-sensor precipitation estimates at finer scale. *J. Hydrometeor.*, **8**, 38–55, https://doi.org/10.1175/JHM560.1.

——, D. T. Bolvin, and E. J. Nelkin, 2010: The TRMM Multi-Satellite Precipitation Analysis (TMPA). *Satellite Rainfall Applications for Surface Hydrology*, F. Hossain and M. Gebremichael, Eds., Springer-Verlag, 3–22.

Jackson, B., S. E. Nicholson, and D. Klotter, 2009: Mesoscale convective systems over western equatorial Africa and their relationship to large-scale circulation. *Mon. Wea. Rev.*, **137**, 1272–1294, https://doi.org/10.1175/2008MWR2525.1.

Jacob, M., A. Frankil, M. Haile, A. Zwertvaegher, and J. Nyssen, 2013: Assessing spatio-temporal rainfall variability in a tropical mountain area (Ethiopia) using NOAA's rainfall estimates. *Int. J. Remote Sens.*, **34**, 8319–8335, https://doi.org/10.1080/01431161.2013.837230.

Joyce, R. J., J. E. Janowiak, P. A. Arkin, and P. Xie, 2004: CMORPH: A method that produces global precipitation estimates from passive microwave and infrared data at high spatial and temporal resolution. *J. Hydrometeor.*, **5**, 487–503, https://doi.org/10.1175/1525-7541(2004)005<0487:CAMTPG>2.0.CO;2.

Kamsu-Tamo, P. H., S. Janicot, D. Monkam, and A. Lenuou, 2014: Convection activity over the Guinen coast and central Africa during northern spring from synoptic to intra-seasonal timescales. *Climate Dyn.*, **43**, 3377–3401, https://doi.org/10.1007/s00382-014-2111-y.

Kizza, M., I. Westerberg, A. Rodhe, and H. K. Ntale, 2012: Estimating areal rainfall over Lake Victoria and its basin using ground-based and satellite data. *J. Hydrol.*, **464–465**, 401–411, https://doi.org/10.1016/j.jhydrol.2012.07.024.

Koutsouris, A. J., D. L. Chen, and S. W. Lyon, 2016: Comparing global precipitation data sets in eastern Africa: A case study of Kilombero Valley, Tanzania. *Int. J. Climatol.*, **36**, 2000–2014, https://doi.org/10.1002/joc.4476.

Laing, A. G., R. E. Carbone, and V. Levizzani, 2011: Cycles and propagation of deep convection over equatorial Africa. *Mon. Wea. Rev.*, **139**, 2832–2853, https://doi.org/10.1175/2011MWR3500.1.

Long, Y., Y. Zhang, and Q. Ma, 2016: A merging framework for rainfall estimation at high spatiotemporal resolution for distributed hydrological modeling in a data-scarce area. *Remote Sens.*, **8**, 599, https://doi.org/10.3390/rs8070599.

Love, T. B., V. Kumar, P. Xie, and W. Thiaw, 2004: A 20-year daily Africa precipitation climatology using satellite and gauge data. *14th Conf. on Applied Meteorology*, Seattle, WA, Amer. Meteor. Soc., P5.4, http://ams.confex.com/ams/pdfpapers/67484.pdf.

Maidment, R. I., D. I. F. Grimes, R. P. Allan, H. Greatrex, O. Rojas, and O. Leo, 2013: Evaluation of satellite-based and model re-analysis rainfall estimates for Uganda. *Meteor. Appl.*, **20**, 308–317, https://doi.org/10.1002/met.1283.

——, and Coauthors, 2017: A new, long-term daily satellite-based rainfall dataset for operational monitoring in Africa. *Sci. Data*, **4**, 170063, https://doi.org/10.1038/sdata.2017.63.

Mashingia, F., F. Mtalo, and M. Bruen, 2014: Validation of remotely sensed rainfall over major climatic regions in northeast Tanzania. *Phys. Chem. Earth*, **67-69**, 55–63, https://doi.org/10.1016/j.pce.2013.09.013.

McCollum, J. R., A. Gruber, and M. B. Ba, 2000: Discrepancy between gauges and satellite estimates of rainfall in equatorial Africa. *J. Appl. Meteor.*, **39**, 666–679, https://doi.org/10.1175/1520-0450-39.5.666.

Munzimi, Y. A., M. C. Hansen, B. Adusei, and G. B. Senay, 2015: Characterizing Congo Basin rainfall and climate using Tropical Rainfall Measuring Mission (TRMM) satellite data and limited rain gauge ground observations. *J. Appl. Meteor. Climatol.*, **54**, 541–555, https://doi.org/10.1175/JAMC-D-14-0052.1.

Negron Juarez, R. I. N., W. H. Li, R. Fu, K. Fernandes, and A. D. Cardoso, 2009: Comparison of precipitation datasets over the tropical South American and African continents. *J. Hydrometeor.*, **10**, 289–299, https://doi.org/10.1175/2008JHM1023.1.

Neupane, N., 2016: The Congo basin zonal overturning circulation. *Adv. Atmos. Sci.*, **33**, 767–782, https://doi.org/10.1007/s00376-015-5190-8.

Nguyen, H., and J. P. Duvel, 2008: Synoptic wave perturbations and convective systems over equatorial Africa. *J. Climate*, **21**, 6372–6388, https://doi.org/10.1175/2008JCLI2409.1.

Nicholson, S. E., 2018: The ITCZ and the seasonal cycle over equatorial Africa. *Bull. Amer. Meteor. Soc.*, **99**, 337–348, https://doi.org/10.1175/BAMS-D-16-0287.1.

——, and J. P. Grist, 2003: The seasonal evolution of the atmospheric circulation over West Africa and equatorial Africa. *J. Climate*, **16**, 1013–1030, https://doi.org/10.1175/1520-0442(2003)016<1013:TSEOTA>2.0.CO;2.

——, and A. K. Dezfuli, 2013: The relationship of interannual variability in western equatorial Africa to the tropical oceans and atmospheric circulation. Part I. The boreal spring. *J. Climate*, **26**, 45–65, https://doi.org/10.1175/JCLI-D-11-00653.1.

——, C. Funk, and A. Fink, 2018a: One and a half centuries of rainfall variability over the African continent. *Global Planet. Change*, **165**, 114–127, https://doi.org/10.1016/j.gloplacha.2017.12.014.

——, D. Klotter, A. K. Dezfuli, and L. Zhou, 2018b: New rainfall data sets for the Congo Basin and surrounding regions. *J. Hydrometeor.*, **19**, 1379–1396, https://doi.org/10.1175/JHM-D-18-0015.1.

Novella, N. S., and W. M. Thiaw, 2013: African Rainfall Climatology version 2 for famine early warning systems. *J. Appl. Meteor. Climatol.*, **52**, 588–606, https://doi.org/10.1175/JAMC-D-11-0238.1.

Pokam, W. M., L. A. T. Djiotang, and F. K. Mkankam, 2012: Atmospheric water vapor transport and recycling in equatorial

Central Africa through NCEP/NCAR reanalysis data. *Climate Dyn.*, **38**, 1715–1729, https://doi.org/10.1007/s00382-011-1242-7.

——, C. L. Bain, R. S. Chadwick, R. Graham, D. J. Sonwa, and F. M. Kamga, 2014: Identification of processes driving low-level westerlies in west equatorial Africa. *J. Climate*, **27**, 4245–4262, https://doi.org/10.1175/JCLI-D-13-00490.1.

Pombo, S., and R. Proença de Oliveira, 2015: Evaluation of extreme precipitation estimates from TRMM in Angola. *J. Hydrol.*, **523**, 663–679, https://doi.org/10.1016/j.jhydrol.2015.02.014.

——, ——, and A. Mendes, 2015: Validation of remote-sensing precipitation products for Angola. *Meteor. Appl.*, **22**, 395–409, https://doi.org/10.1002/met.1467.

Samba, G., and D. Nganga, 2012: Rainfall variability in Congo-Brazzaville: 1932–2007. *Int. J. Climatol.*, **32**, 854–873, https://doi.org/10.1002/joc.2311.

——, ——, and M. Mpounza, 2008: Rainfall and temperature variations over Congo-Brazzaville between 1950 ad 1998. *Theor. Appl. Climatol.*, **91**, 85–97, https://doi.org/10.1007/s00704-007-0298-0.

Sandjon, A. T., A. Nzeukou, and C. Tchawoua, 2012: Intraseasonal atmospheric variability and its interannual modulation in central Africa. *Meteor. Atmos. Phys.*, **117**, 167–179, https://doi.org/10.1007/s00703-012-0196-6.

——, ——, ——, F. M. Kamga, and D. Vondou, 2014a: A comparative analysis of intraseasonal atmospheric variability in OLR and 1DD GPCP rainfall data over central Africa. *Theor. Appl. Climatol.*, **116**, 37–49, https://doi.org/10.1007/s00704-013-0911-3.

——, ——, ——, B. Sonfack, and T. Siddi, 2014b: Comparing the patterns of 20–70 days intraseasonal oscillations over central Africa during the last three decades. *Theor. Appl. Climatol.*, **118**, 319–329, https://doi.org/10.1007/s00704-013-1063-1.

Schneider, U., A. Becker, P. Finger, A. Meyer-Christoffer, B. Rudolf, and M. Ziese, 2015: GPCC Full Data Monthly Product version 7 at 2.5°: Monthly land-surface gauges built on GTS-based and historic data. DWD, accessed December 2017, https://doi.org/10.5676/DWD_GPCC/FD_M_V7_250.

Serrat-Capdevila, A., M. Merino, J. B. Valdes, and M. Durcik, 2016: Evaluation of the performance of three satellite precipitation products over Africa. *Remote Sens.*, **8**, 836, https://doi.org/10.3390/rs8100836.

Sinclaire, Z., A. Lenouo, C. Tchawoua, and S. Janicot, 2015: Synoptic Kelvin type perturbation waves over Congo basin over the period 1979–2010. *J. Atmos. Terr. Phys.*, **130–131**, 43–56, https://doi.org/10.1016/j.jastp.2015.04.015.

Sorooshian, S., K. Hsu, D. Braithwaite, H. Ashouri, and the NOAA CDR Program, 2014: NOAA Climate Data Record (CDR) of Precipitation Estimation from Remotely Sensed Information using Artificial Neural Networks (PERSIANN-CDR), version 1 revision 1. Subset used: Monthly rainfall over Africa, NOAA National Centers for Environmental Information. accessed December 2017, https://doi.org/10.7289/V51V5BWQ.

Soula, S., J. K. Kasereka, J. F. Georgis, and C. Barthe, 2016: Lightning climatology in the Congo basin. *Atmos. Res.*, **178–179**, 304–319, https://doi.org/10.1016/j.atmosres.2016.04.006.

Sun, Q., C. Miao, Q. Duan, H. Ashouri, S. Sorooshian, and K.-L. Hsu, 2018: A review of global precipitation data sets: Data sources, estimation, and intercomparisons. *Rev. Geophys.*, **56**, 79–107, https://doi.org/10.1002/2017RG000574.

Tarnavsky, E., D. Grimes, R. Maidment, E. Black, R. P. Allan, and M. Stringer, 2014: Extension of the TAMSAT satellite-based rainfall monitoring over Africa and from 1983 to present. *J. Appl. Meteor. Climatol.*, **53**, 2805–2822, https://doi.org/10.1175/JAMC-D-14-0016.1.

Taylor, K. E., 2001: Summarizing multiple aspects of model performance in a single diagram. *J. Geophys. Res.*, **106**, 7183–7192, https://doi.org/10.1029/2000JD900719.

Todd, M. C., and R. Washington, 2004: Climate variability in central equatorial Africa: Influence from the Atlantic sector. *Geophys. Res. Lett.*, **31**, L23202, https://doi.org/10.1029/2004GL020975.

van de Giesen, N., R. Hut, and J. Selker, 2014: The Trans-African Hydro-Meteorological Observatory (TAHMO). *Wiley Interdiscip. Rev.: Water*, **1**, 341–348, https://doi.org/10.1002/wat2.1034.

Vondou, D. A., A. Nzeukou, A. Lenouo, and F. M. Kamga, 2010a: Seasonal variations in the diurnal patterns of convection in Cameroon–Nigeria and the neighboring areas. *Atmos. Sci. Lett.*, **11**, 290–300, https://doi.org/10.1002/asl.297.

——, ——, and F. M. Kamga, 2010b: Diurnal cycle of convective activity over the West of Central Africa based on Meteosat images. *Int. J. Appl. Earth Obs. Geoinf.*, **12** (Suppl. 1), S58–S62, https://doi.org/10.1016/j.jag.2009.09.011.

Xie, P., and P. A. Arkin, 1996: Analyses of global monthly precipitation using gauge observations, satellite estimates, and numerical model predictions. *J. Climate*, **9**, 840–858, https://doi.org/10.1175/1520-0442(1996)009<0840:AOGMPU>2.0.CO;2.

——, and ——, 1997: Global precipitation: A 17-year monthly analysis based on gauge observations, satellite estimates, and numerical model outputs. *Bull. Amer. Meteor. Soc.*, **78**, 2539–2558, https://doi.org/10.1175/1520-0477(1997)078<2539:GPAYMA>2.0.CO;2.

——, R. J. Joyce, S. Wu, S.-H. Yoo, Y. Yarosh, F. Sun, and R. Lin, 2017: Reprocessed, bias-corrected CMORPH CRT global high resolution estimates form 1998. *J. Hydrometeor.*, **18**, 1617–1641, https://doi.org/10.1175/JHM-D-16-0168.1.

Yin, X., and A. Gruber, 2010: Validation of the abrupt change in GPCP precipitation in the Congo River basin. *Int. J. Climatol.*, **30**, 110–119, https://doi.org/10.1002/joc.1875.

——, ——, and P. Arkin, 2004: Comparison of the GPCP and CMAP merged gauge-satellite monthly precipitation products for the period 1979–2001. *J. Hydrometeor.*, **5**, 1207–1222, https://doi.org/10.1175/JHM-392.1.

Zebaze, S., A. Lenuou, and C. Tchawoua, 2017: Interaction between moisture transport and Kelvin waves over Equatorial Africa through ERA-Interim. *Atmos. Sci. Lett.*, **18**, 300–306, https://doi.org/10.1002/asl.756.

Zhou, L., and Coauthors, 2014: Widespread decline of Congo rainforest greenness in the past decade. *Nature*, **509**, 86–90, https://doi.org/10.1038/nature13265.

Zipser, E. J., D. J. Cecil, C. T. Liu, S. W. Nesbitt, and D. P. Yorty, 2006: Where are the most intense thunderstorms on Earth? *Bull. Amer. Meteor. Soc.*, **87**, 1057–1071, https://doi.org/10.1175/BAMS-87-8-1057.